

AD-A160 672

ANALYSIS OF THE DYNAMICS AND CONTROL OF A TWO DEGREE OF
FREEDOM ROBOTIC MANIPULATOR MOUNTED ON A MOVING BASE
(U) ARMY MILITARY PERSONNEL CENTER ALEXANDRIA VA

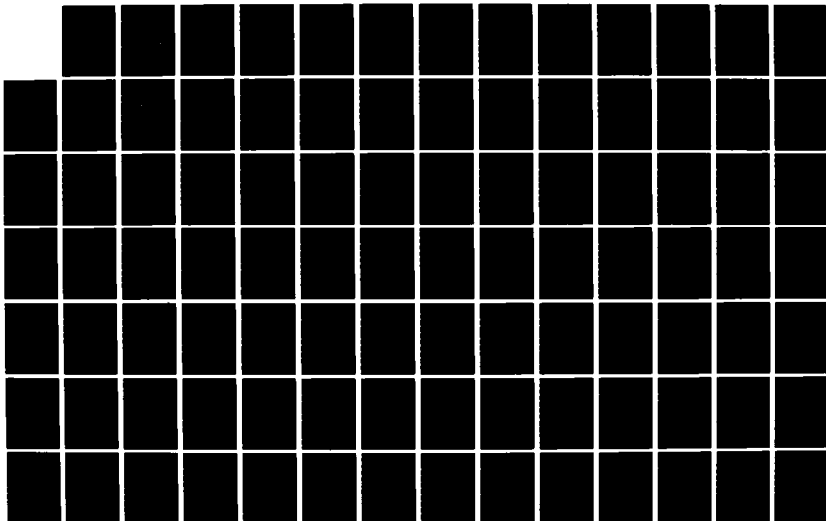
1/2

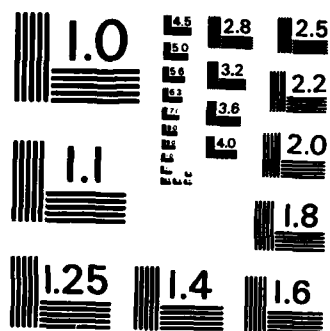
UNCLASSIFIED

R LYNCH 18 OCT 85

F/G 5/8

NL





MICROCOPY RESOLUTION TEST CHART
NATIONAL BUREAU OF STANDARDS-1963-A

(2)

AD-A160 672

Not Entered)

IN PAGE

READ INSTRUCTIONS
BEFORE COMPLETING FORM

2. GOVT ACCESSION NO.

3. RECIPIENT'S CATALOG NUMBER

4. TITLE (and Subtitle)

Analysis of the Dynamics and Control
of a Two Degree of Freedom Robotic Manipulator
Mounted on a Moving Base

5. TYPE OF REPORT & PERIOD COVERED

Final Report
18 Oct 85

6. PERFORMING ORG. REPORT NUMBER

7. AUTHOR(s)

CPT Ricky Lynch

8. CONTRACT OR GRANT NUMBER(s)

9. PERFORMING ORGANIZATION NAME AND ADDRESS

Student
HQDA, Milpercen (DAPC-OPA-E)
200 Stovall Street, Alexandria VA 22332

10. PROGRAM ELEMENT, PROJECT, TASK
AREA & WORK UNIT NUMBERS

11. CONTROLLING OFFICE NAME AND ADDRESS

HQDA, Milpercen
ATTN: (DAPC-OPA-E)
200 Stovall Street Alexandria VA 22332

12. REPORT DATE

18 Oct 85

13. NUMBER OF PAGES

118

14. MONITORING AGENCY NAME & ADDRESS (if different from Controlling Office)

15. SECURITY CLASS. (of this report)

unclassified

15a. DECLASSIFICATION/DOWNGRADING
SCHEDULE

16. DISTRIBUTION STATEMENT (of this Report)

Approved for public release; distribution unlimited

17. DISTRIBUTION STATEMENT (of the abstract entered in Block 20, if different from Report)

18. SUPPLEMENTARY NOTES

Thesis, Massachusetts Institute of Technology

19. KEY WORDS (Continue on reverse side if necessary and identify by block number)

20. ABSTRACT (Continue on reverse side if necessary and identify by block number)

(over)

DTIC

ELECTE

OCT 29 1985

B

DTIC FILE COPY

Mounting a robotic manipulator on a moving base creates numerous control problems due to the hostile dynamics created as a result of the disturbances due to base motion. This thesis studies a realistic ~~app~~ military application of a robotic manipulator, that of a robotic tank autoloader. Attempts are made to control the manipulator by conventional control algorithms (such as PID control) and by more advanced control strategies (LQR, Decoupling and Pole placement). It is shown that these control techniques are not able to compensate for the motion of the base, and recommendations of possible solutions to the problem are made.



Approved	
NTIS	<input checked="" type="checkbox"/>
DTIC	<input type="checkbox"/>
Unavail	<input type="checkbox"/>
Just	
By	
Distribution	
Availability Codes	
Dist	
A-1	

Analysis of the Dynamics and Control of a Two Degree of Freedom
Robotic Manipulator Mounted on a Moving Base

CPT Ricky Lynch
HQDA, MILPERCEN (DAPC-OPA-E)
200 Stovall Street
Alexandria, VA 22332

Final Report 18 October 1985

Approved for public release; distribution unlimited

A thesis submitted to The Massachusetts Institute of Technology
in partial fulfillment for the degree of Master of Science

05 04 6

ANALYSIS OF
THE DYNAMICS AND CONTROL OF A
TWO DEGREE OF FREEDOM
ROBOTIC MANIPULATOR
MOUNTED ON A MOVING BASE

BY

RICKY LYNCH
B.S., UNITED STATES MILITARY ACADEMY
(1977)

SUBMITTED IN PARTIAL FULFILLMENT OF THE
DEGREE OF

MASTER OF SCIENCE

AT THE

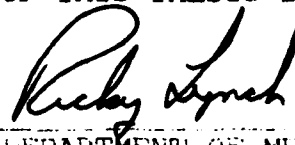
MASSACHUSETTS INSTITUTE OF TECHNOLOGY

OCTOBER 18, 1985

(C) RICKY LYNCH 1985

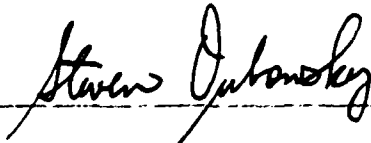
THE AUTHOR HEREBY GRANTS TO M.I.T. PERMISSION TO REPRODUCE
AND TO DISTRIBUTE COPIES OF THIS THESIS DOCUMENT IN WHOLE OR
IN PART.

SIGNATURE OF AUTHOR



DEPARTMENT OF MECHANICAL ENGINEERING
OCTOBER 18, 1985

CERTIFIED BY



STEVEN DUBOWSKY
THESIS ADVISOR

ACCEPTED BY



AIN A. SONIN
CHAIRMAN, DEPARTMENTAL GRADUATE COMMITTEE

ANALYSIS OF
THE DYNAMICS AND CONTROL OF A
TWO DEGREE OF FREEDOM
ROBOTIC MANIPULATOR
MOUNTED ON A MOVING BASE

by

RICKY LYNCH

Submitted to the Department of Mechanical Engineering
on October 18, 1985 in partial fulfillment of the
requirements for the Degree of Master of Science.

ABSTRACT

Much of the current state of the art technology for the dynamics and control of robotic manipulators is geared primarily towards industrial applications. Industrial manipulators usually operate in well structured environments, i.e. mounted on fixed bases working with known parameters such as payloads, etc. Mounting robotic manipulators on moving bases offers the potential of greatly extending the manipulator applications. However, the motion of the base creates a number of problems in terms of the control of the manipulator. The base motion subjects the manipulator to large scale disturbances that can seriously degrade system performance. This thesis illustrates the problems associated with a moving base as it applies to a two degree of freedom manipulator. It is shown that conventional control techniques, such as PID control, cannot effectively compensate for the base accelerations in a typical application. It is also shown that more advanced control algorithms, including decoupling control, LQR control, and pole placement prove to be ineffective to varying degrees. The linear controller that had the best results, the one designed utilizing a pole placement technique, is then applied to the complete nonlinear system in an attempt to investigate the influence of the base motion over the entire range of motion of the manipulator. Recommendations for possible solutions to the moving base, problem, along with recommendations for extensions of this work, are then made.

Thesis Advisor: Dr. Steven Dubowsky
Professor of Mechanical Engineering

PREFACE

This thesis is submitted to the Department of Mechanical Engineering, Massachusetts Institute of Technology as the final requirement for obtaining the Master of Science Degree.

The author would like to take this opportunity to thank all those personnel at M.I.T. who provided so much insight into the problems associated with mounting a robotic manipulator on a moving base. Their thoughtfulness and engineering expertise proved to be very helpful. In particular I would like to thank Mr. Zia Vafa for his assistance throughout my studies. He was always available to answer questions and to provide encouragement.

I would like to thank Professor Steven Dubowsky for his encouragement and understanding throughout my thesis work. He proved to be an enlightened mentor and an inspiration. His perseverance and dedication to his profession insured that I learn and understand the subject matter, not just memorize it.

I would especially like to thank my wife Sarah, and my children Susan and Lucas. Their patience and understanding throughout my studies at M.I.T. enabled me to work on my thesis without feeling as if I was neglecting my family. This thesis would not have been possible without their love and support. They were always there with a smile and a hug when I needed it.

TABLE OF CONTENTS

LIST OF FIGURES.....	6
CHAPTER 1 - INTRODUCTION	
1.1 Introduction.....	8
1.2 Outline of thesis work.....	11
1.3 Detailed description of moving base problem.....	14
1.4 Description of status of current research.....	15
CHAPTER 2 - DETERMINATION OF MODEL PARAMETERS	
2.1 Introduction.....	17
2.2 Design of model.....	17
2.3 Model for base acceleration.....	26
2.4 Specifications for system performance.....	28
2.4 Summary.....	30
CHAPTER 3 - DEVELOPMENT OF EQUATIONS OF MOTION	
3.1 Description of Lagrangian technique.....	31
3.2 Use of Absolute Coordinate System.....	32
3.3 Development of Equations of Motion.....	32
3.4 Nonlinear Simulation of Equations	38
3.5 Linearization of Equations of Motion.....	44
3.6 State-Space Representation of Equations.....	46
3.7 Summary	47
CHAPTER 4 - APPLICATION OF CONVENTIONAL CONTROL STRATEGIES	
4.1 Discussion of PID Control Strategy.....	48
4.2 Development of linear controller.....	50
4.3 Summary.....	64
CHAPTER 5 - ADVANCED CONTROL STRATEGIES	
5.1 Discussion of Advanced Control Strategies.....	65
5.2 Decoupling Control.....	66
5.3 LQR Control.....	75
5.4 Pole Placement Technique.....	82
5.5 Summary.....	90
CHAPTER 6 - NONLINEAR SIMULATION OF POLE PLACE CONTROLLER	
6.1 Introduction.....	91
6.2 Nonlinear Simulation Results.....	91
6.3 Summary.....	96
CHAPTER 7 - CONCLUSIONS.....	
CHAPTER 8 - RECOMMENDATIONS FOR FURTHER RESEARCH.....	
LIST OF REFERENCES.....	101
APPENDIX A -Non-Linear Simulation Routines.....	
MBAS.T.....	105
SYST.T.....	106
REGNON.T.....	107

CREGNON.T.....	108
APPENDIX B - LINEARIZATION SPECIFICS.....	109
Linearized Equations of Motion.....	110
Program LINEAR.....	112
APPENDIX C - POLESYS3 Example Routine.....	113

LIST OF FIGURES

FIGURE	TITLE	PAGE NUMBER
1-1	Human Operator as a Tank Loader.....	12
2-1	Model Design.....	18
2-2	Manipulator Workspace Dimensions.....	20
2-3	Models for Links.....	21
2-4	Mass Distribution for Links.....	24
2-5	Table of Model Parameters.....	25
2-6	Model of Base Acceleration.....	27
2-7	Shape of Typical Tank Ammunition.....	29
3-1	System Representation.....	31
3-2	System Velocity Components.....	34
3-3	Generalized Forces.....	36
3-4	Nonlinear Simulation # 1.....	39
3-5	Nonlinear Simulation # 2.....	40
3-6	Nonlinear Simulation # 3.....	41
3-7	Nonlinear Simulation # 4.....	42
3-8	Nonlinear Simulation # 5.....	43
4-1	PID Control Block Diagram.....	49
4-2	Nominal Values for Linear Controller.....	51
4-3	PID Control With Small Gains.....	57
4-4	PID Control With Larger Gains.....	58
4-5	PID Control of Link Two.....	59
4-6	Bode Plot of PID Controller With Small Gains..	60
4-7	Bode Plot of PID Controller With Larger Gains.	61
4-8	PID Control Response to Base Disturbance.....	63
5-1	Decoupling Control Block Diagram.....	68
5-2	Decoupled Control for Link One.....	72

5-3	System Decoupling Control.....	73
5-4	Decoupled Control Response to Base Motion.....	74
5-5	LQR Control First Attempt.....	79
5-6	LQR Control Without Base Motion.....	80
5-7	LQR Control Response to Base Motion.....	81
5-8	Possible Pole Locations.....	82
5-9	Open Loop Pole Locations.....	84
5-10	Pole Place Control Without Base Motion.....	86
5-11	Pole Place Control Response to Base Motion....	87
5-12	Pole Place Control Response to Base Motion.... 2nd Attempt	88
5-13	Pole Place Control Response to Base Motion.... 3rd Attempt	89
6-1	Nonlinear Simulation Without Base Motion.....	93
6-2	Nonlinear Simulation With Base Motion.....	94
6-3	Nonlinear Simulation With Base Motion..... Smaller Bandwidth	95

CHAPTER 1

INTRODUCTION

1.1 Introduction

Robotics is a technology that is moving into many realms of today's society, particularly in the area of industrial manufacturing. State-of-the-art technology allows us to build and program robotic devices and manipulators that can perform many of the tasks that are currently being accomplished by human operators. This has proven to be extremely useful in those tasks that are inherently dangerous to human operators, and those that are mundane and repetitive.

In addition to the obvious industrial applications, robotics has a role to play in today's military. In fact, a study by a committee appointed by the National Academies of Science and Engineering in the early 1980's identified numerous military tasks that could be performed by robotic systems [1]. These included a tank autoloader, a robotic sentry, and various ammunition handling devices. A basic problem is the fact that the technology that enables us to build industrial manipulators is not directly transferrable to manipulators that would operate in a military environment.

Today's industrial manipulators are designed to work under highly structured and "friendly" conditions. They are mounted on stationary, relatively rigid bases. They are programmed to complete highly specified tasks in which most often the parameters (particularly the payload parameters) are

relatively well known [2]. In contrast, manipulators in military applications would be forced to work in a "hostile" dynamic environment in which many critical system parameters would be constantly changing. In order to accomplish many military missions, the robotic manipulator would have to be mounted on a moving base. Moving bases would enable manipulators to be transported throughout their areas of operation. The utility of these systems could be maximized if the manipulator could operate both while the base is moving and after the base arrives at the new location.

Two relatively simple prospective examples which would involve manipulators mounted on moving bases are a tank autoloader and a manipulator mounted on the back of a truck to handle ammunition. The tank autoloader would be used to load main gun rounds in the gun tube of a tank. The manipulator mounted on the back of a truck would perform such tasks as picking up pallets of ammunition, breaking open the pallets, and repackaging the ammunition into smaller, user oriented packages. There is an important technical difference between these two applications that must be addressed. In the tank autoloader problem the motion of the manipulator would have no effect on the tank itself, primarily due to the mass difference between the two objects. On the other hand, the motion of the manipulator mounted on the back of a truck would cause the truck itself to move, which would create additional dynamic problems.

In such military applications these moving bases would possess significant suspension flexibility that could seriously degrade system performance. Although outriggers could possibly be used to reduce this base flexibility, they would probably not be sufficient to negate all flexibility problems. When the vehicle or base is in a transportation mode, the manipulator would be subject to large dynamic disturbance forces that would also tend to degrade performance. In addition this base motion would excite the structural resonances of the manipulator causing additional problems. Another major problem facing manipulators working in a military environment would be the large payload range that the manipulators might need to handle. For example, if a manipulator was to be used as an automatic loader for a tank, the weight of the payload would vary from forty to sixty pounds depending upon the type of shell. These payload variations would also degrade performance.

In order to bring robotic technology to the point where robotic manipulators can be used in a military environment, the above problems, in addition to others, need to be solved. This thesis focuses on some of the dynamics and control problems encountered when the manipulator is mounted on a moving base. The disturbances that the manipulator is subject to as a result of the base motion are studied, and various control strategies are investigated to determine how well they compensate for the base disturbances.

1.2 Outline of thesis work

In order to fully understand the dynamics and control problems of mobile manipulators, it is essential to first determine what effects large base motions have on their performance. This is done by using dynamic simulations. To conduct meaningful simulations which include the dynamic nonlinearities, a system with realistic characteristics is designed. The model was designed with a realistic application in mind, that of the tank autoloader. Payload parameters, actuator restrictions, cycle time and geometric constraints all were considered. For the purpose of this research a two link, two degree of freedom manipulator was modelled by simulation. The manipulator links were assumed to be rigid. Only planar motion was considered.

It is important at this point to understand the tasks that a robotic manipulator serving as a tank autoloader would have to perform. Figure 1-1 shows the current tank loader, a human operator [30]. The loader stands inside the tank turret, and during the loading sequence he reaches to the rear to extract a round out of the ammunition storage area (ready rack). He then pivots and loads the round into the gun tube. A manipulator designed to perform this mission would operate in the same mode in basically the same workspace.



FIGURE 1-1 HUMAN OPERATOR AS TANK LOADER

Once the system for the autoloader application was designed, the nonlinear equations of motion were developed using the Lagrangian technique. A nonlinear simulation was then conducted in order to determine the extent of the problem. In addition, a nonlinear simulation at this point in the analysis provided for an opportunity to check the response of the modelled system against anticipated response based on engineering experience.

The nonlinear equations of motion were then linearized around selected nominal values. This was done to provide for linearized equations of motion for which linear controllers could be designed. Analysis of linearized equations allowed

for investigation of the system without nonlinear complications. The linear controllers designed were then, by definition, effective for small perturbations around the selected nominal values.

Conventional control strategies were then applied to the linearized system to study their effectiveness in compensating for the base motion. In the analysis, the system was first modelled as a manipulator being mounted on a fixed base. A controller was then designed that met operating specifications. The model was then changed to provide for motion of the base, and the linear controller that had proved to be effective for the fixed base problem was then applied to the system with base motion. A PID controller was first developed and investigated, but it was unable to effectively compensate for the motion of the base. More advanced control algorithms were then applied to the problem, using the same procedure described above. They also proved to be ineffective in compensating for the base motion, although some had more success than the others. The advanced control algorithms studied included decoupling control, LQR control, and a pole placement technique.

At this point the linear controller that had the best results was then applied to the full nonlinear system to study it's effectiveness over the entire range of motion of the manipulator, taking into account all of the nonlinear complications. As with the linear control design, the controllers effectiveness was first studied as applied to a

manipulator in the absence of base motion, and then base motion was added to the system. It was found that the controller was indeed effective in the absence of base motion, but was unable to compensate for the motion of the base.

1.3 Detailed description of the moving base problem

The motion of the base creates many dynamics and control problems for the manipulator. The large inertial disturbance forces that are generated by the motion of the base create a hostile dynamic environment for the manipulator. These dynamic disturbances are similar to those one feels when he is in an elevator while the elevator accelerates or decelerates. Even though the elevator control panel and the individual are moving in the same reference frame, an individual has a certain degree of difficulty reaching out to push a control button while the elevator is starting or stopping. Another good example would be the disturbances one feels when he is in an automobile traveling down a bumpy road. Reaching out to pull out the cigarette lighter or turn the radio on can become difficult as a result of the base motion. In addition, the motion of the base could excite the manipulator's structural resonances. This could severely degrade system performance.

The results shown in this thesis indicate that conventional control techniques cannot effectively control a manipulator mounted on a moving base. In addition it is shown that more advanced control algorithms are also ineffective. It is suggested that effective controllers could possibly be

designed if the controller had access to sensory information that would indicate the motion of the base. This sensory information could be provided by sophisticated linear accelerometers capable of an extremely high sampling rate. The base velocity could then be determined by integration routines.

1.4 Description of status of current research

Research in the realm of robotic devices and manipulators to date has been focused on design and control of industrial robots. As a result, the "moving base" problem has recieved little attention. Soviet engineers are investigating the problem to a certain degree, however. They have recently focused on the problem of how to mathematically model a manipulator mounted on a moving platform. Their published work to date has focused on modelling considerations and does not address the issue of appropriate control strategies [3].

A large amount of current research regarding the dynamics and control of robotic manipulators can indirectly be applied to the "moving base" issue, however. The Luh-Walker-Paul algorithm that is designed to compute the forces and torques necessary to control a manipulator along a planned path provides for the inclusion of base motion in the computation of required torques [4]. The required torques can then be dynamically fed forward (inverse dynamics) in an attempt to compensate for the motion of the base. Cannon's work on end point control could be applied to the "moving base" issue by

focusing on the exact location of the end point in relation to the target regardless of the base motion [5].

In addition, there has been work in areas that are peripheral to the problem of mounting a manipulator on a moving base. Research is being done at the Rensselaer Polytechnic Institute in regards to operating a robot in constrained work volume, as would be the problem with a tank autoloader. This work concentrates on the trajectory problem that is a function of the control strategy selected [27]. Researchers at the University of Iowa are concentrating on techniques to model the dynamics of a vehicle with flexible and rigid components intermixed. This research illustrates what effect bumpy terrain has on the vibrating motion of a vehicle, which in turn would effect the manipulator mounted on the vehicle [28]. In the area of military vehicles, models have been developed that predict dynamic track loads on vehicles that navigate cross-country [29].

In summary, research in the area of the dynamics and control of a robotic manipulator mounted on a moving base is sparse at best. Little has been done to date to determine what effect base motion has on the control of the manipulator, and whether or not conventional control algorithms can effectively compensate for the base motion.

CHAPTER 2

DETERMINATION OF MODEL PARAMETERS

2.1 Introduction

It is imperative in investigating the problems associated with the dynamics and control of a robotic manipulator mounted on a moving platform that the researcher consider realistic applications. As was mentioned before, there exists numerous potential applications for the mobile robot within the military. This thesis will focus on the concept of mounting a robotic manipulator inside a tank to load ammunition. This will allow for selection of realistic model parameters in addition to identifying acceptable performance specifications.

1.2 Design of Model

Modeling is a critical aspect of engineering analysis. A designer can take an extremely complex real system and, utilizing appropriate design procedures, develop a model that will emulate the performance of the actual system. It is important to design the model to be as simple as possible by making certain simplifying assumptions so that the significant system behavior can be analyzed. However, the model must clearly represent the behavior of the actual system, and avoid oversimplifications which result in misleading conclusions.

The model used for this research was a two degree of freedom, two link planar manipulator. The design of the model is as indicated in figure 2-1:

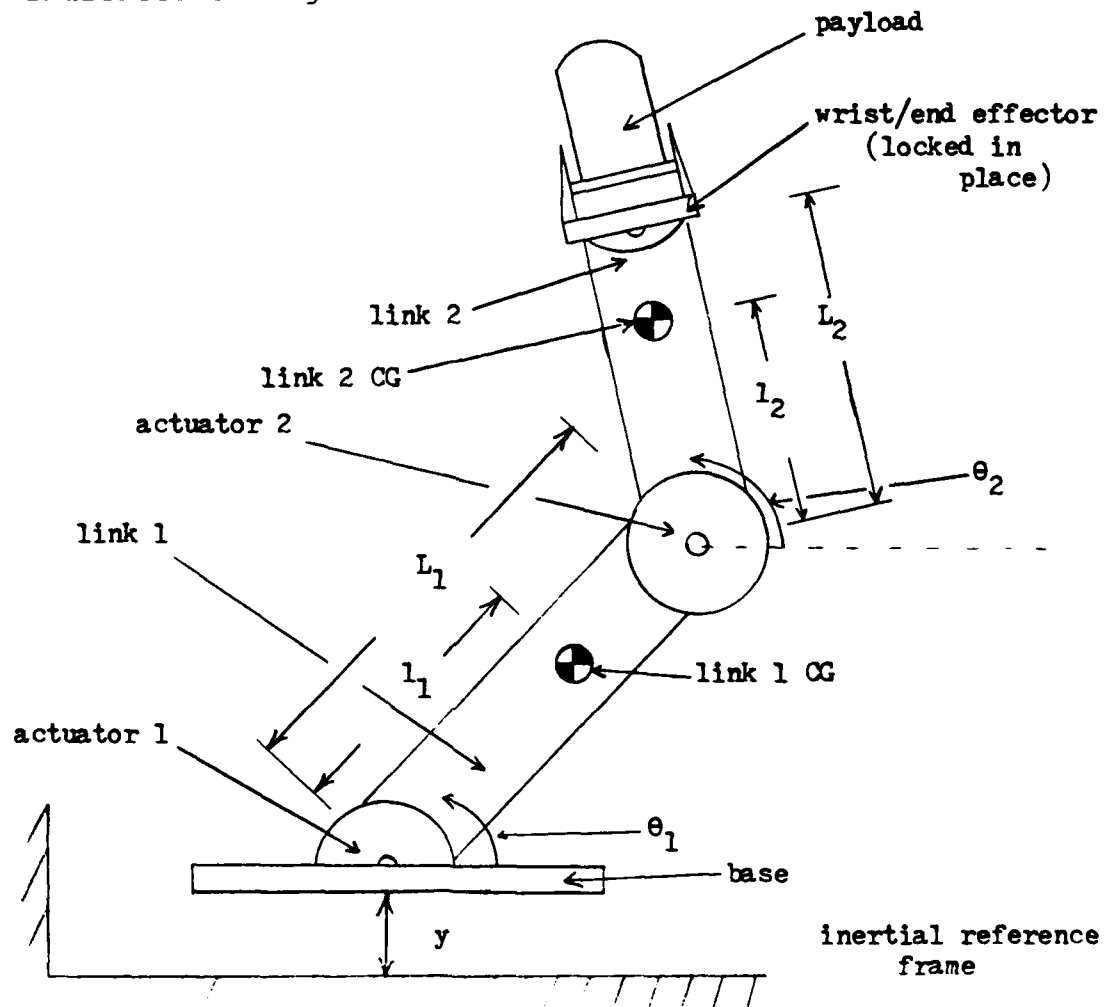


FIGURE 2-1 MODEL DESIGN

Certain assumptions are made in order to insure that the model was as simple as possible but still emulated the important actual system behavior. These included:

- (1) The motion of the manipulator is restricted to planar motion.

(2) The manipulator is rigidly fixed to its moving base.

(3) The links of the manipulator are assumed to be thin walled hollow steel tubes. The center of mass of the links is located along the link center line. The links are assumed to be rigid.

(4) The actuators and end effector are included in the model for mass distribution purposes only. All motor backlash effects, etc. were neglected.

In order to determine model parameters, the use of the system had to be considered. The fact that this design was intended as a tank autoloader resulted in the following assumptions:

(1) The payload that this manipulator would handle would vary from forty to sixty pounds.

(2) The work space dimensions and hence the size of the links for the manipulator are consistent with the size of the tank turret. These dimensions are indicated in the following illustration:

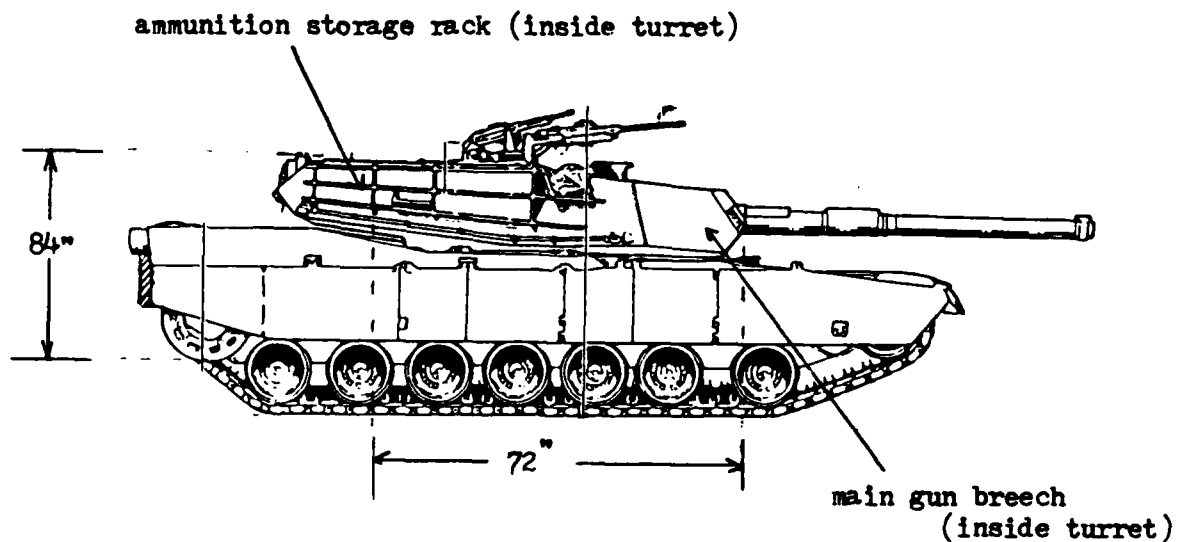


FIGURE 2-2 MANIPULATOR WORKSPACE DIMENSIONS

This workspace dictates that the height of the manipulator when in a vertical position can be no more than seven feet. In addition, the manipulator trajectory must be able to include the path from the ammunition rack to the gun tube.

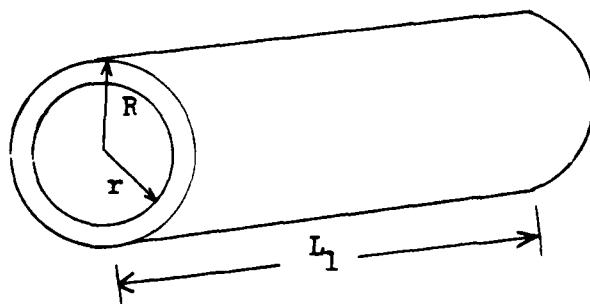
At this point the system parameters can be determined. This is done in the following manner:

STEP 1 - MASS PARAMETERS

The thickness of the walls of the thin walled hollow steel tube forming the links is dictated by the assumption that the links would be effectively rigid. The natural frequencies of the links must be high enough so that the motion of the base

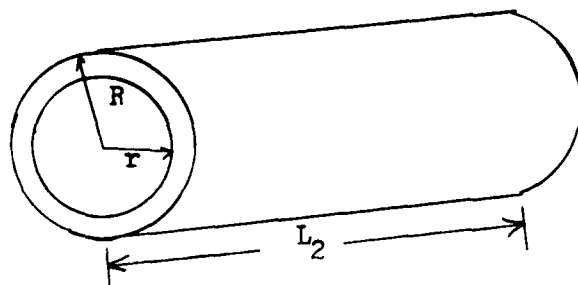
does not excite them, and the structural resonances of the links do not interact with the manipulator's control system. The link parameters were calculated in the following manner:

link 1



$$\begin{aligned} R &= 4.5'' \\ r &= 3.5'' \\ L_1 &= 36'' \end{aligned}$$

link 2



$$\begin{aligned} R &= 4.0'' \\ r &= 3.0'' \\ L_2 &= 36'' \end{aligned}$$

FIGURE 2-3 MODELS FOR LINKS

$$\text{Volume Calculations: } V = R^2 L - r^2 L \quad (2.1)$$

$$V_1 = 904.76 \text{ in}^3$$

$$V_2 = 791.70 \text{ in}^3$$

$$\text{Density of steel} = .284 \text{ lb/in}^3$$

Therefore:

$$\text{Weight link 1} = 904.76 \times .284 = 257.0 \text{ lbs}$$

$$\text{Weight Link 2} = 791.7 \times .284 = 224.8 \text{ lbs}$$

The motor actuators have to be included in order to include all of the mass elements to locate the link's center of mass. Due to the relatively heavy payloads, it was assumed that hydraulic rotary actuators would be used. A study of commercially available rotary actuators capable of performing designated tasks determined that suppliers such as Bird-Johnson marketed actuators that would suffice [33]. These Bird-Johnson actuators are Model HYD-R0-AC, and have the following representative characteristics:

ACTUATOR 1= 80 lbs, max torque 20,000 in-lbs

ACTUATOR 2= 30 lbs, max torque 5,000 in-lbs. In terms of mass distribution it was assumed that the weight of the actuators would be distributed throughout the links in the following manner:

Weight of actuator 1: 75% on platform, 25% on the lower end of link 1

Weight of actuator 2: 66% on link 1, 37% on the lower end of link 2

In addition, a commercially available end effector that would handle the prescribed payloads was found that weighed 25 lbs. The end effector will be mounted as shown in figure 2-1.

Based on the above calculations and assumptions, mass calculations can now be made:

MASS of link 1= total weight on link 1/acceleration due to gravity

$$= 297/32.2 = 9.2 \text{ slugs}$$

MASS of link 2 (with 60lb payload)= total weight on link 2 + payload/ acceleration due to gravity

$$= 319.8 / 32.2 = 9.93 \text{ slugs}$$

MASS of link 2 (without payload)= total weight on link 2/ acceleration due to gravity

$$= 259.8 / 32.2 = 8.07 \text{ slugs}$$

STEP 2- CALCULATION OF CENTER OF MASS LOCATIONS

The location of the center of mass for each link can be determined by using the following formula:

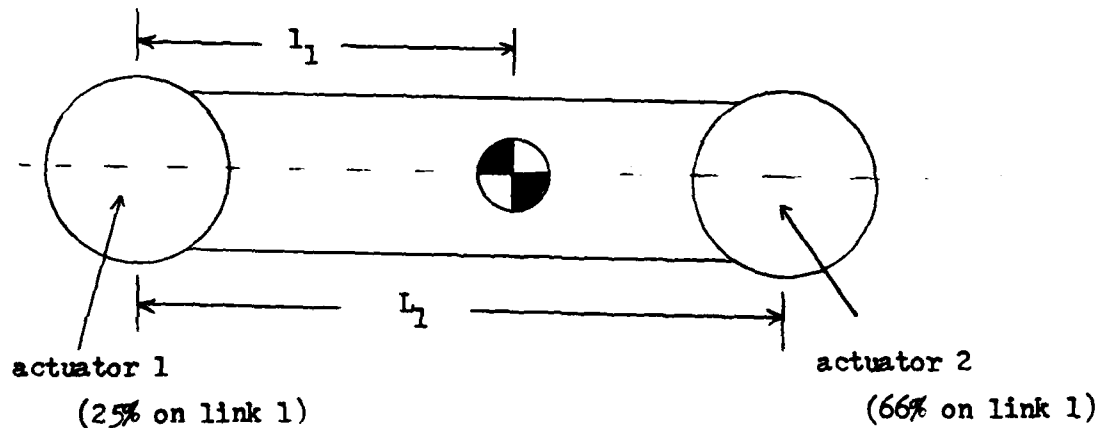
$$l_{ic} = \frac{\sum m_i \times r_i}{m_i} \quad (2.2)$$

where:

m_i = mass of each link (including actuators, etc.)

r_i = distance to mass position
i

link 1



link 2

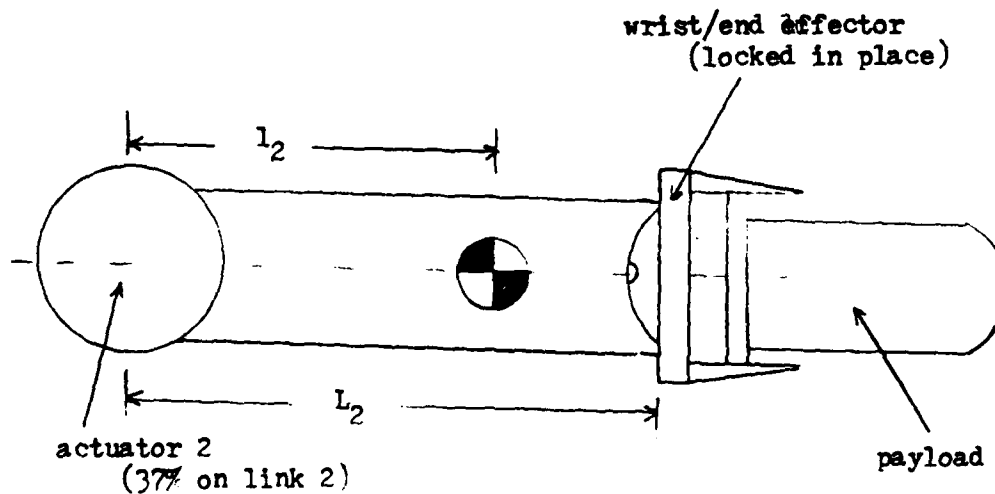


FIGURE 2-4 MASS DISTRIBUTION FOR LINKS

Which leads to the following parameters:

$$l_{1c} = 18.4"$$

$$l_{2c} = 22.6" \text{ (with payload)}$$

$$l_{2c} = 15.7" \text{ (without payload)}$$

STEP 3- CALCULATION OF MASS MOMENT OF INERTIA

The mass moment of inertia can be thought of as a measure of the link's resistance to rotational motion. It is evaluated about an axis passing through the object's center of gravity. The values for the moment of inertia about each link are as follows:

$$J_{\text{link 1}} = 6.44 \text{ lbf-sec}^2 / \text{ft}$$

$$J_{\text{link 2}} = 5.11 \text{ lbf-sec}^2 / \text{ft}$$

All calculated parameters are presented in the following table:

	mass (m) slugs	link length (L) feet	center of mass (l) feet	m.o.i. (J) lbf-sec ² /ft
link 1	9.2	3	1.53	6.44
link 2 (with payload)	9.93	3	1.88	5.11
link 2 (w/o payload)	8.07	3	1.31	5.11

FIGURE 2-5 TABLE OF MODEL PARAMETERS

2.3 Model for base acceleration

It is also important to effectively model base accelerations. The base accelerations that the model is subjected to must closely simulate the type of accelerations that tank moving cross country would experience. Due to the irregularity of ground conditions, combined with the high rate of speed of today's tanks (45 mph), the tank would be subject to random input accelerations of relatively high magnitude. For the purposes of this thesis only vertical accelerations will be considered. Past experiments have indicated that maximum vertical accelerations would be of the order of 16 ft/sec², approximately one half the acceleration due to gravity [7]. This value will be used as the maximum value for the base disturbances to the test manipulator. The input will be modeled as a random "white noise" input, with the simulation returning a random scalar between 16 and -16 for each time step (see figure 2-6). As is evident in figure 2-6, the model chosen for the base acceleration is indeed "white noise" with a zero mean. Random inputs in the range of acceptable values are generated.

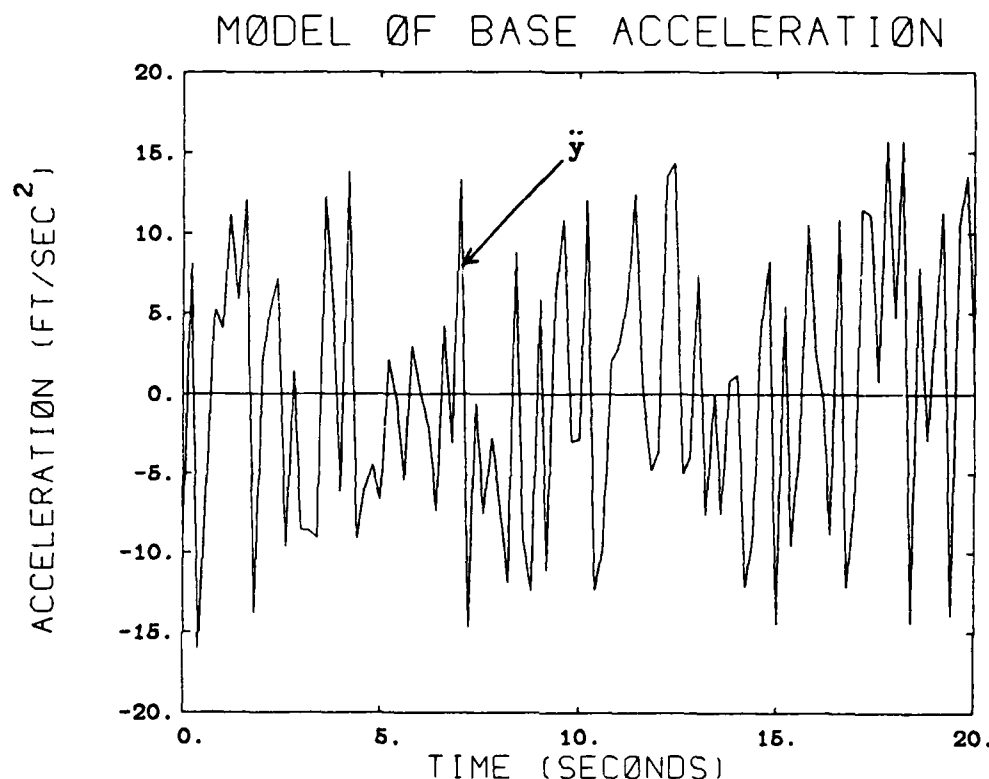


FIGURE 2-6 MODEL OF BASE ACCELERATION

It is important to have an understanding of what this input entails, and to understand the bandwidth of this disturbance. By definition, white noise has a very high bandwidth. Bandwidth is roughly proportional to the speed of response [12]. The faster the speed of response, the higher the bandwidth. As is indicated in figure 2-6, the model that is being used for the base acceleration has an extremely high

bandwidth, i.e. the speed of response is very fast. In the creation of this model a sampling time of .2 seconds was used. Observation of the model, along with application of the sampling theorem, indicate that the bandwidth of this model is of the order of 10 hertz [10]. This fact becomes extremely important in control design, and will be addressed in more detail later.

2.4 Specifications for system performance

As was indicated earlier, selection of a realistic application for the system design provides for concrete specifications of system performance. These specifications will be used to evaluate the effectiveness of control design. For control design, specifications are needed in the areas of response time, accuracy and stability.

In terms of response time, in order for a controlled system to be considered effective its response time must be at least as fast as a human operator. Speed of response in loading the tank ammunition is a critical parameter, the quickest system must be utilized. A well trained human operator can extract the ammunition from the ammunition rack, pivot, and load the round into the gun tube in five seconds. Hence, the manipulator must be able to move from its initial position to the desired position in less than five seconds.

In terms of accuracy, the ammunition round must slide into the gun tube. The fact that the ammunition is tapered at the top (see figure 2-7) allows the ammunition to basically guide itself into the gun tube once the ammunition point is inside the gun breach.

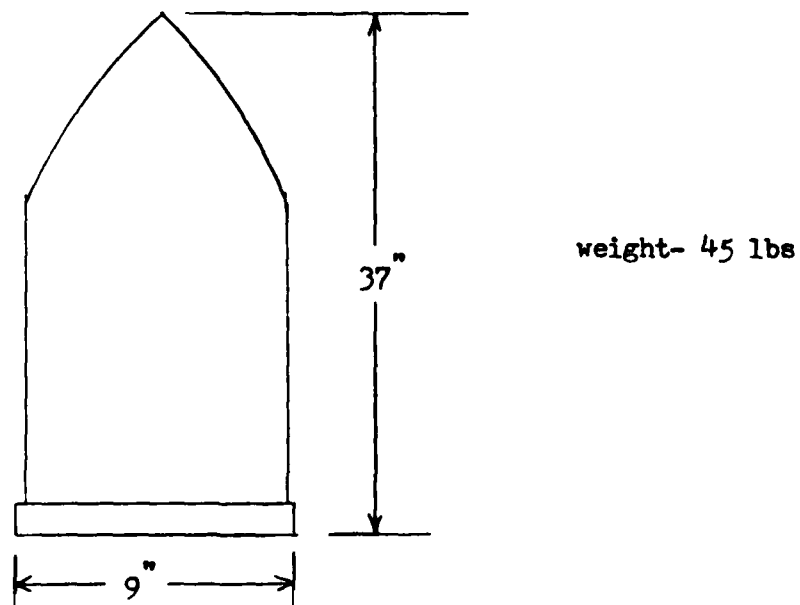


FIGURE 2-7 SHAPE OF TYPICAL TANK AMMUNITION

This allows for a slight flexibility in terms of position accuracy for the end effector of the manipulator. Based on the size of the gun tube breach, the flexibility amounts to a range of plus or minus 3 inches in final end effector position. In the design of the two-link manipulator being studied, the end effector location is a function of both the joint angles, θ_1 and θ_2 (see figure 2-1). Thus, both angles must be considered in determining position accuracy. By trigonometric transformation, the range of flexibility in the

endpoint location transforms to approximately an allowable deviation of plus or minus .05 radians in the steady state values for θ_1 and θ_2 .

Transient response and stability are additional important specifications. The manipulator must have reached a stable configuration by the time the ammunition round arrives at the gun tube. Wild oscillations at that point could result in the round prematurely detonating inside the gun turret.

2.5 Summary

In this chapter, a model to emulate the real system performance was designed. A realistic application for the device was selected, and model parameters were calculated with this application in mind. The model was kept as simple as possible, with emphasis on concentrating on a specific aspect of behavior, response to the base acceleration. The base acceleration itself was modeled in such a manner as to closely emulate that acceleration tank a moving tank would experience. These model parameters will now be used in dynamic simulations. The system performance specifications were determined in order to evaluate controller effectiveness.

CHAPTER 3

DEVELOPMENT OF THE EQUATIONS OF MOTION

3.1 Description of Lagrangian technique

The next step is to develop the equations of motion for the model described in the previous chapters. In this thesis the Lagrangian formalism is utilized in developing these equations. The Lagrangian formalism is based upon variational mechanics, where work and energy stored into the system must be identified. Workless forces such as holonomic constraint forces at each of the joints do not appear in the formulation. The equations of motion are written in terms of generalized coordinates and generalized forces. The system to be investigated is as shown in figure 3-1:

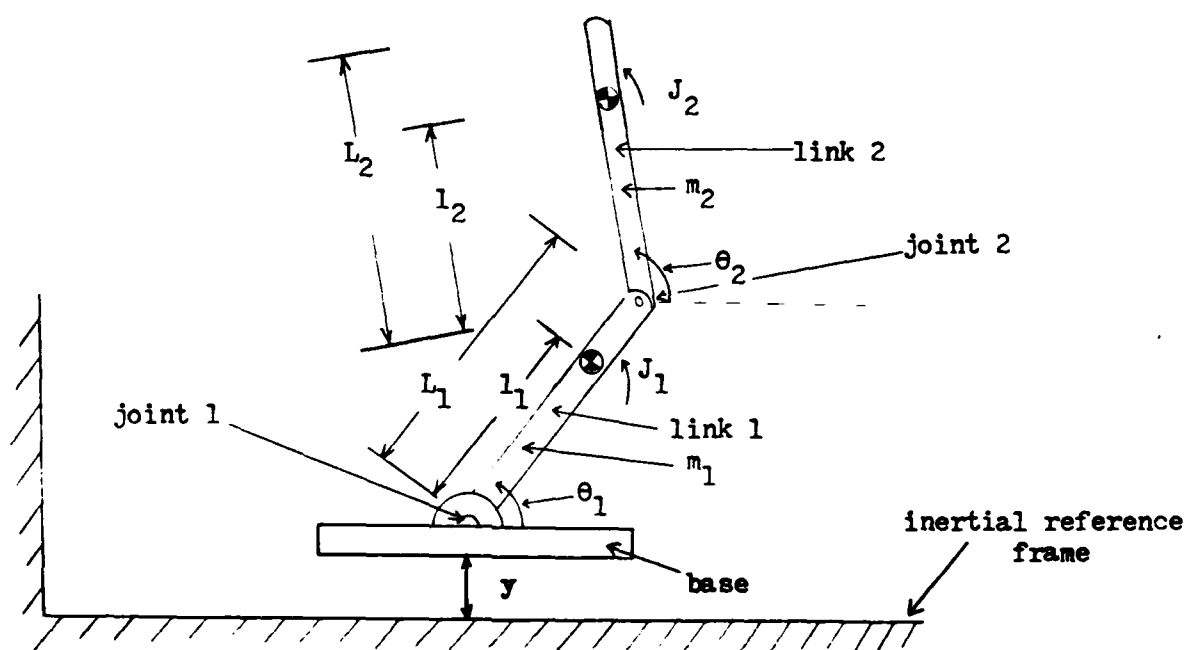


FIGURE 3-1 SYSTEM REPRESENTATION

3.2 Use of absolute coordinate system

Note the use of absolute generalized coordinates for the joint angles, θ_1 and θ_2 , shown in figure 3-1. Both angles are measured relative to an inertial reference frame. This is an important point. Usually manipulator joint angles are expressed in terms of relative angles, i.e. the angles are measured relative to the link to which they are attached. This is primarily due to the fact that position encoders work with relative angles. Absolute coordinates were chosen in this thesis due to the fact that the resulting equations of motion are simpler (less terms) [8].

3.3 Development of equations of motion

The Lagrangian formalism is based on the equation:

$$\frac{d}{dt} \left[\frac{\partial T}{\partial \dot{q}_i} \right] - \frac{\partial T}{\partial q_i} + \frac{\partial V}{\partial q_i} = Q_i \quad (3.1)$$

where: T = kinetic energy

V = potential energy

q_i = generalized coordinates (θ_1 and θ_2)

Q_i = generalized forces

In this case the generalized coordinates are θ_1 and θ_2

as shown in figure 3-1. Initially one must evaluate the system's energy terms:

KINETIC ENERGY

The kinetic energy for the entire system is the sum of the kinetic energy of each of the two links. Knowing that the expression for the kinetic energy of a rigid body is:

$$T = 1/2 m v^2 + 1/2 J w^2 \quad (3.2)$$

where: m = the mass of the body

v = the linear velocity of the body (center of mass)

J = the body's mass moment of inertia

w = the angular velocity of the body (internal)

The system's kinetic energy can now be expressed in the following manner:

$$T = 1/2 m_1 \left| \frac{v}{c1} \right|^2 + 1/2 J_1 \dot{\theta}_1^2 + 1/2 m_2 \left| \frac{v}{c2} \right|^2 + 1/2 J_2 \dot{\theta}_2^2 \quad (3.3)$$

where:

$\left| \frac{v}{c1} \right|^2$ = the magnitude of the velocity of center mass of link one with respect to inertial reference frame

$\left| \frac{v}{c2} \right|^2$ = the magnitude of the velocity of center mass of link two with respect to inertial reference frame

m_1 = the mass of link 1

m_2 = the mass of link 2
(with or without the payload)

J_1 = the mass moment of inertia of link 1

J_2 = the mass moment of inertia of link 2
(with or without the payload)

Determining the components of the velocity vectors for each of the two links is illustrated below:

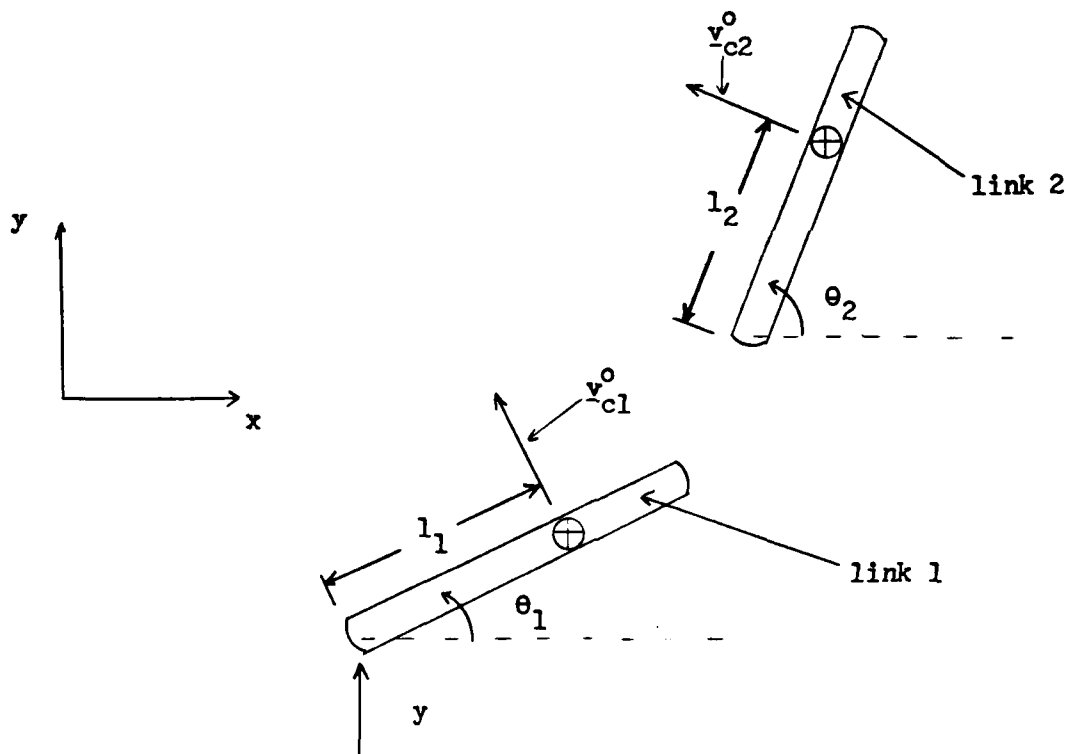


FIGURE 3-2 SYSTEM VELOCITY COMPONENTS

As depicted in figure 3-2, the velocity components can now be expressed as:

$$\frac{v}{c1} = \begin{bmatrix} \dot{\theta} \sin \theta \\ \dot{y} + \dot{\theta} \cos \theta \end{bmatrix} \quad (3.4)$$

$$\frac{v}{c2} = \begin{bmatrix} L \dot{\theta} \sin \theta + l_2 \dot{\theta} \sin \theta \\ \dot{y} + L \dot{\theta} \cos \theta + l_2 \dot{\theta} \cos \theta \end{bmatrix} \quad (3.5)$$

The magnitude of the velocity components can now be substituted back into equation (3.4) to arrive at an expression for the system's total kinetic energy.

POTENTIAL ENERGY

The potential energy of the system is due to gravity and can be found from the well known relationship:

$$V = \sum_i m_i g h_i \quad (3.6)$$

where:

m_i = mass of link i

h_i = height of the center of mass of link i above the reference frame

An examination of the geometry indicated in figure 3-1 leads to the following expression for the system's potential energy:

$$V = m_1 g y_1 + m_1 g l_1 \sin \theta_1 + m_2 g y_2 + m_2 g L_1 \sin \theta_1 + m_2 g l_2 \sin \theta_2 \quad (3.7)$$

COMPUTATION OF GENERALIZED FORCES

The generalized forces are the non-conservative forces acting within the system [31]. In this case the non-conservative forces are the torques applied to the actuators as shown below:

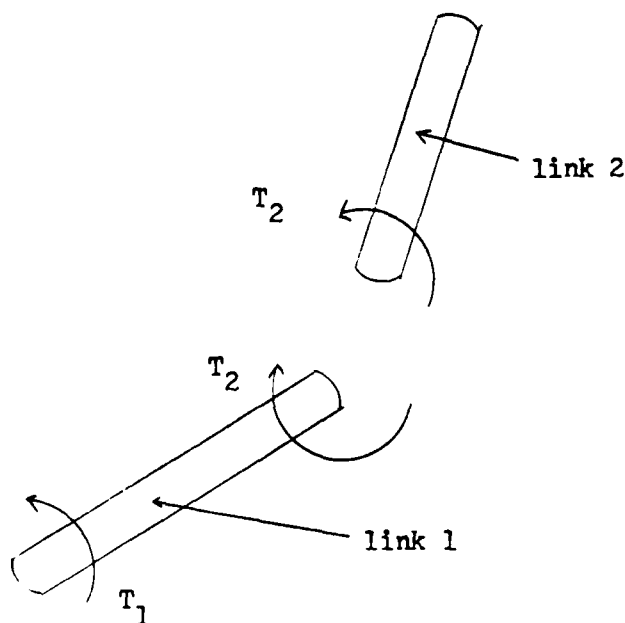
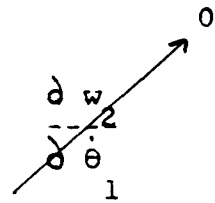


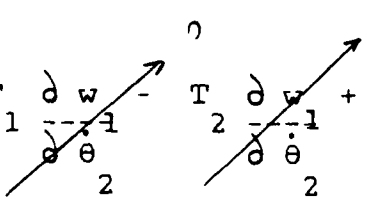
FIGURE 3-3 GENERALIZED FORCES

Analysis of the above illustration leads to:

$$Q_1 = T_1 \frac{\partial w_1}{\partial \dot{\theta}_1} - T_2 \frac{\partial w_1}{\partial \dot{\theta}_1} + T_2 \frac{\partial w_2}{\partial \dot{\theta}_1}$$


where $\dot{\theta}_1 = \dot{w}_1$; $\dot{\theta}_2 = \dot{w}_2$

$$Q_1 = T_1 - T_2$$

$$Q_2 = T_1 \frac{\partial w_1}{\partial \dot{\theta}_2} - T_2 \frac{\partial w_1}{\partial \dot{\theta}_2} + T_2 \frac{\partial w_2}{\partial \dot{\theta}_2}$$


$$Q_2 = T_2$$

(3.9)

Reference [18] contains a detailed description of the relationship between the generalized forces. The task is now to substitute the energy and generalized forces terms back into equation 3.1, and take the successive derivatives as indicated. The result is the following equations of motion for the system:

$$\begin{aligned} & (m_1 l_1^2 + J_1 + m_2 L_1^2) \ddot{\theta}_1 + m_2 L_1 l_2 \cos(\theta_2 - \theta_1) \ddot{\theta}_2 \\ & + (m_1 l_1 \cos \theta_1 + m_2 L_1 \cos \theta_2) \ddot{y} - m_1 l_1 \dot{\theta}_1 \sin \theta_1 \dot{\theta}_1 \\ & - m_2 L_1 l_2 \sin(\theta_2 - \theta_1) \dot{\theta}_1^2 + (m_1 l_1 \cos \theta_1 + m_2 L_1 \cos \theta_2) g \\ & = T_1 - T_2 \end{aligned} \quad (3.10)$$

$$\begin{aligned}
& \frac{m}{2} \frac{L}{1} \frac{1}{2} \cos(\theta - \theta_1) \ddot{\theta}_1 + \left(\frac{m}{2} \frac{L}{2} + J \right) \ddot{\theta}_2 + \frac{m}{2} \frac{L}{2} \cos \theta \ddot{y}_2 \\
& + \frac{m}{2} \frac{L}{1} \frac{1}{2} \sin(\theta - \theta_1) \dot{\theta}_1^2 + \frac{m}{2} g \frac{L}{2} \cos \theta \\
& = T_2
\end{aligned} \tag{3.11}$$

3.4 Nonlinear Simulation of Equations of Motion

The resulting equations of motion are obviously highly nonlinear. In order to determine what effect various base accelerations have on the system itself in the absence of control a nonlinear simulation was conducted. In addition, a simulation at this point allows for testing of the model. Predictable simulation results leads to increased confidence in the model. Various simulations were conducted to check model response. The nonlinear simulations were conducted via the SIMNON package [7] utilizing a fourth order Runge-Kutta integration routine. The results of the simulations are indicated below:

SIMULATION # 1

The first simulation is conducted in the absence of any external forces. Gravity is set to zero, and no external torques are applied. The base is stationary. Initial conditions for the joint angles were:

$$\begin{aligned}\theta_1 &= .5 \text{ radians} \\ \theta_2 &= 1.0 \text{ radians}\end{aligned}\tag{3.12}$$

The results are as shown:

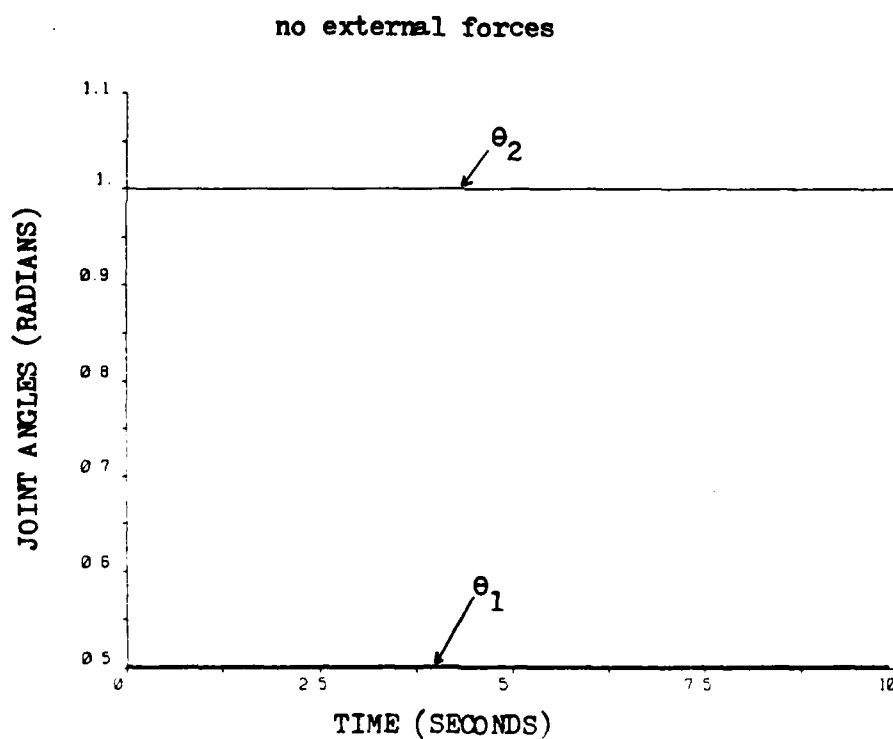


FIGURE 3-4 NONLINEAR SIMULATION # 1

These results are as expected. The joint angles remain constant in the absence of any external forces.

SIMULATION # 2

In the second simulation, gravitational forces were considered. Initial conditions for the joint angles were the same as in the first simulation. The results are indicated below:

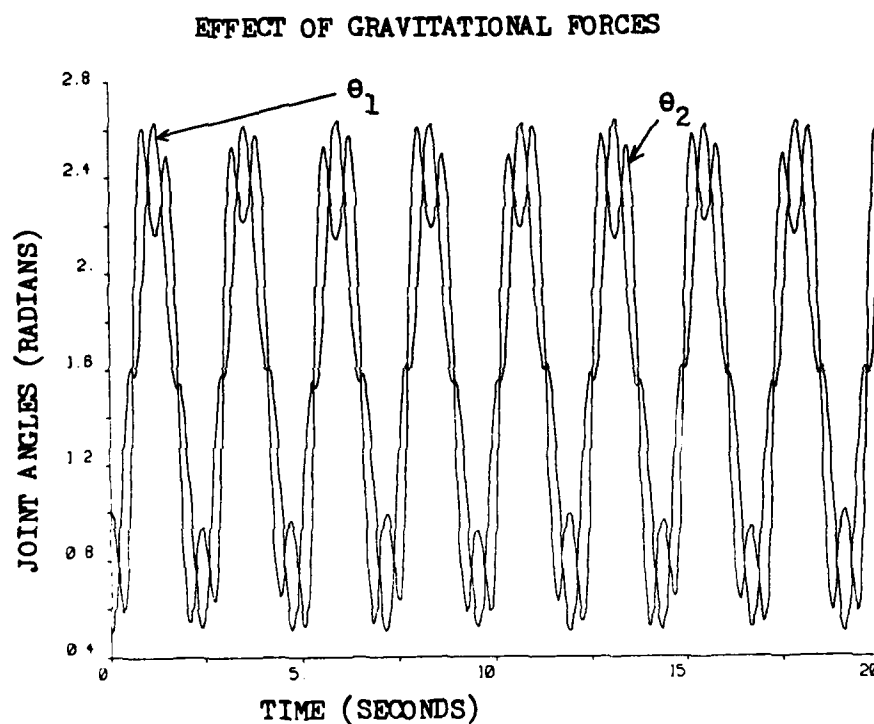


FIGURE 3-5 NONLINEAR SIMULATION #2

In the presence of gravity, the manipulator acts as a double pendulum, swinging with anticipated oscillations. Due to the fact that the model does not contain any damping or friction forces, the oscillation continues indefinitely. These results

were also as expected and lead to increased confidence in the equations of motion.

SIMULATION # 3

In this simulation a constant base acceleration of $16 \text{ ft} / \text{sec}^2$ is applied to the system. All other parameters remain the same as in simulation 2. The results are indicated below:

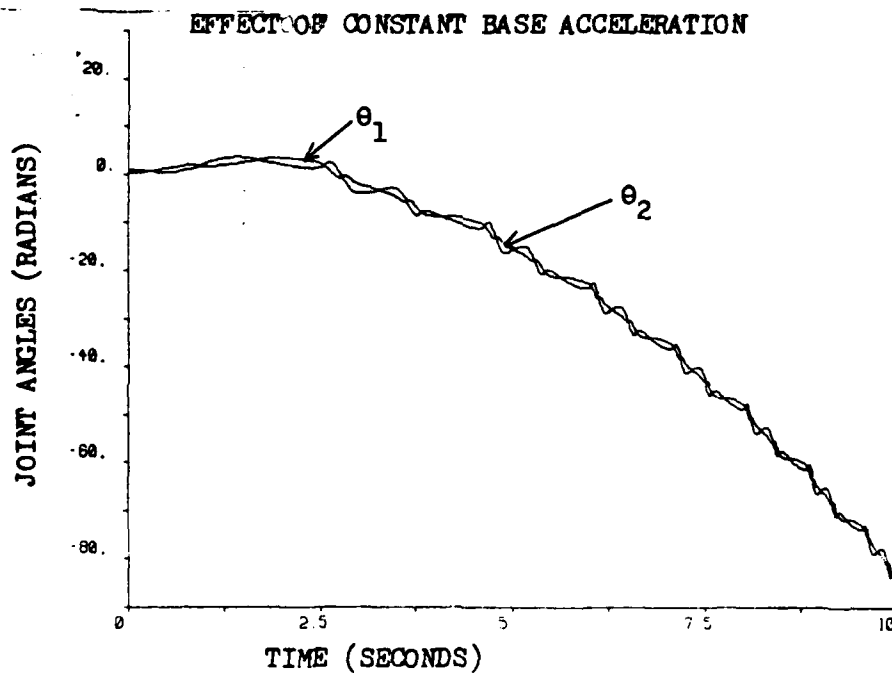


FIGURE 3-6 NONLINEAR SIMULATION # 3

These results are also as anticipated. The constant base acceleration causes the joint angles to fall, and the constant buildup of the acceleration forces causes the manipulator joint angles to whirl.

SIMULATION # 4

In this simulation a sinusoidal base acceleration ($16 \sin 3t$) was applied to the system. The system initial conditions remain the same, and gravity is taken into consideration. The results follow:

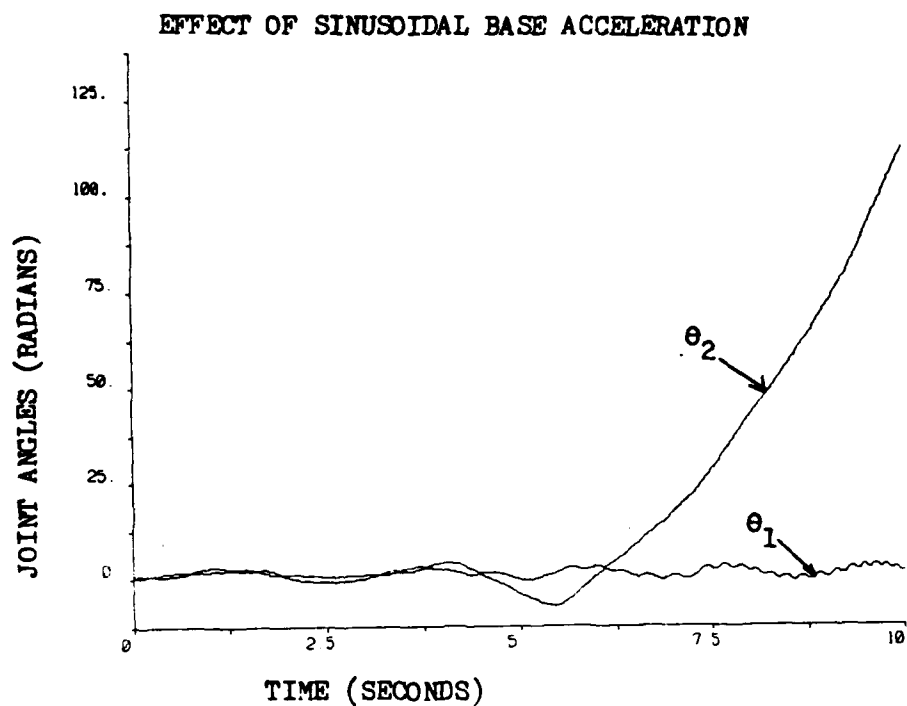


FIGURE 3-7 NONLINEAR SIMULATION #4

The results are also predictable. The joint angles vary as a function of the base acceleration.

SIMULATION #5

This simulation is conducted to test the importance of manipulator configuration in the analysis. The initial

conditions for the joint angles were changed to:

$$\theta_1 = 1.57 \text{ radians}$$

$$\theta_2 = 1.57 \text{ radians}$$

The manipulator is now in a totally vertical position, with both arms sticking straight up. A constant base acceleration of 16 ft/sec^2 is applied, with the following results:

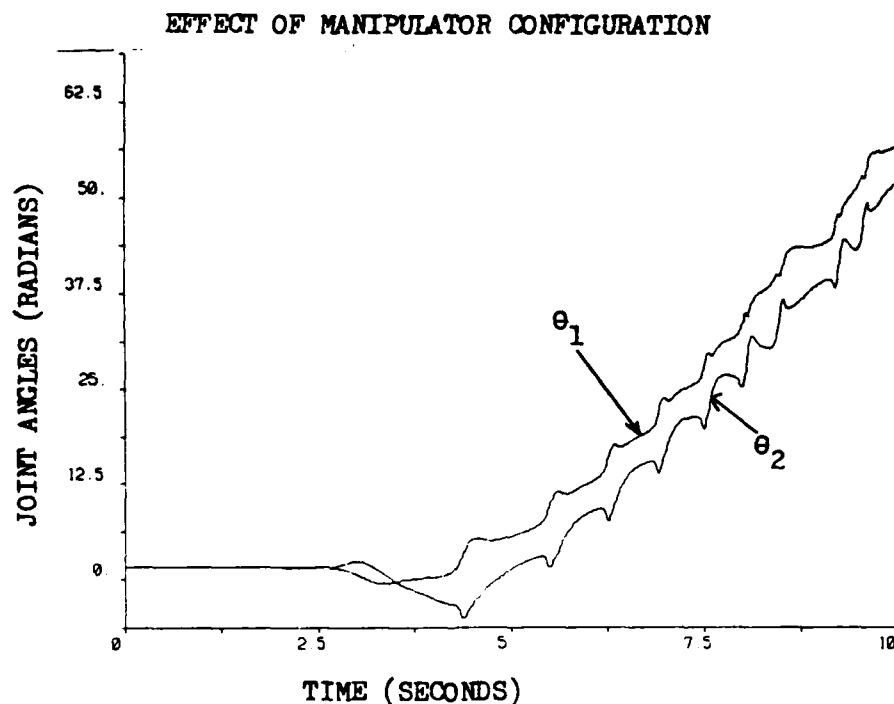


FIGURE 3-8 NONLINEAR SIMULATION #5

This simulation illustrates the importance of manipulator configuration. The joint angles remain at 1.57 radians, as was anticipated, until such a point that the computation roundoff errors caused the manipulator to fall from its vertical position and become influenced by the base

acceleration.

As a further check on the accuracy of the equations of motion, a check on the system's kinetic energy was conducted. In the absence of any external forces, the system's kinetic energy should remain constant. Numerical simulations that checked the kinetic energy of the system were conducted. The system's kinetic energy did remain constant in the absence of external forces, which added credibility to the equations of motion.

3.5 Linearization of Equations of Motion

As was stated earlier, the actual equations of motion are highly nonlinear. It is possible to linearize these equations about selected nominal operating points, and to then design a linear controller for the linearized equations that will insure system stability. In most cases, the nonlinear system will be at least asymptotically stable for small deviations from the selected operating points [9]. The nonlinear system basically behaves like a linear system in a "small neighborhood" about the operating points [10].

The procedure for linearization involved considering small perturbations about selected operating points based on the following definitions:

$$\theta_i = \theta_i^n + \delta \theta_i$$

$$\dot{\theta}_i = \dot{\theta}_i^n + \delta \dot{\theta}_i \quad (3.13)$$

$$\ddot{\theta}_i = \ddot{\theta}_i^n + \delta \ddot{\theta}_i$$

where: θ_i^n , $\dot{\theta}_i^n$, $\ddot{\theta}_i^n$ are selected nominal values

for each joint, and

$\delta \theta_i$, $\delta \dot{\theta}_i$, $\delta \ddot{\theta}_i$ are small perturbations
about the nominal values

Since $\delta \theta_i$, $\delta \theta_j$ are small perturbations from selected nominal values, the following assumptions can be made:

$$\cos(\delta \theta_i) = 1 \quad (3.14)$$

$$\sin(\delta \theta_i) = \delta \theta_i \quad (3.15)$$

$$(\delta \theta_i)(\delta \theta_j) = 0 \quad (3.16)$$

It is important to understand this linearization process. Nominal values are selected that best represent system performance. In terms of engineering analysis it is possible to linearize about specific operating points with the links being stationary (i.e. $\dot{\theta}_1^n = \ddot{\theta}_1^n = 0$), or about specified trajectories with some nominal link velocity and acceleration.

The linearized equations of motion are listed in Appendix B. The actual linearization process entails a great deal of mathematical manipulation. To expedite the process a FORTRAN program (LINEAR) was written that returns the specific numerical coefficients for each of the system variables. (see APPENDIX B).

3.6 State Space Representation of Equations of Motion

The linearized equations can now be written in state-space form. The equations will be represented in the following configuration:

$$\dot{\underline{x}} = \bar{\underline{A}} \underline{x} + \bar{\underline{B}} \underline{u} + \bar{\underline{\Gamma}} \underline{w} \quad (3.17)$$

$$\underline{y} = \bar{\underline{C}} \underline{x} + \bar{\underline{D}} \underline{u} \quad (3.18)$$

where: (1) \underline{x} represents a vector of the states of the system. The states are those variables that are required to completely represent the system in a mathematical model. In this case:

$$\begin{aligned} \underline{x}^T &= [x_1, x_2, x_3, x_4, x_5] \quad (3.19) \\ &= [\delta\theta_1, \delta\dot{\theta}_1, \delta\theta_2, \delta\dot{\theta}_2, \dot{y}] \end{aligned}$$

(2) \underline{u} is a vector of the inputs to the system. In this case:

$$\begin{aligned} \underline{u}^T &= [u_1, u_2] \quad (3.20) \\ &= [T_1, T_2] \end{aligned}$$

where T_1, T_2 are the actuator torques for each of the joints.

(3) \underline{w} is a vector of the disturbances to the system. In this case:

$$\underline{w} = [\ddot{y}] \quad (3.21)$$

- (4) $\underline{\bar{A}}, \underline{\bar{B}}, \underline{\bar{C}}, \underline{\bar{D}},$ and $\underline{\bar{\Gamma}}$ are matrices which contain the actual dynamics of the system. Their numerical values are determined by the coefficients of the system's states as described in equation 3.19.

3.7 Summary

In this chapter the equations of motion for the system under investigation were developed utilizing a Lagrangian technique. Nonlinear simulations of the equations of motion were then conducted to test system response and to determine what effect the base motion had on the system itself. A technique for linearizing the equations of motion was then developed. The linearized equations were then placed into state space form. At this point the controllers can be designed in an attempt to achieve acceptable response.

CHAPTER 4

APPLICATION OF CONVENTIONAL CONTROL STRATEGY

4.1 Discussion of PID control strategy

Current industrial manipulators utilize controllers that are intentionally simple, reliable and easy to implement. The majority of industrial manipulators are controlled by constant gain linear feedback control systems [2]. Typically, these controllers attempt to control the manipulator by using local, decoupled proportional-integral-derivative (PID) controllers at each joint. They are able to accomplish position control, i.e. they can move the manipulator to the configuration that they desire. However these controllers tend to ignore the nonlinear dynamics of the system, and hence tend to be extremely sensitive to disturbances. In addition the performance of industrial controllers is also limited due to restricted sensory capability. They utilize only position and velocity sensors. The question at this point becomes whether or not these commercially available controllers would be effective in controlling the manipulator mounted on a moving base. If individual joint PID controllers are effective in this situation, then the entire problem can be simplified.

PID control is a combination of proportional, derivative and integral control action [12]. The equation of a controller with this combined action is given by:

$$m(t) = K_p e(t) + K_d \dot{e}(t) + K_i \int e(t) dt \quad (4.1)$$

where: $e(t)$ = system error (actual - desired values)

K_p = position error gain

K_d = derivative error gain

K_i = integral error gain

or the transfer function:

$$\frac{M(s)}{E(s)} = \frac{K_p + K_d s + K_i}{s}$$

which is indicated in the following block diagram:

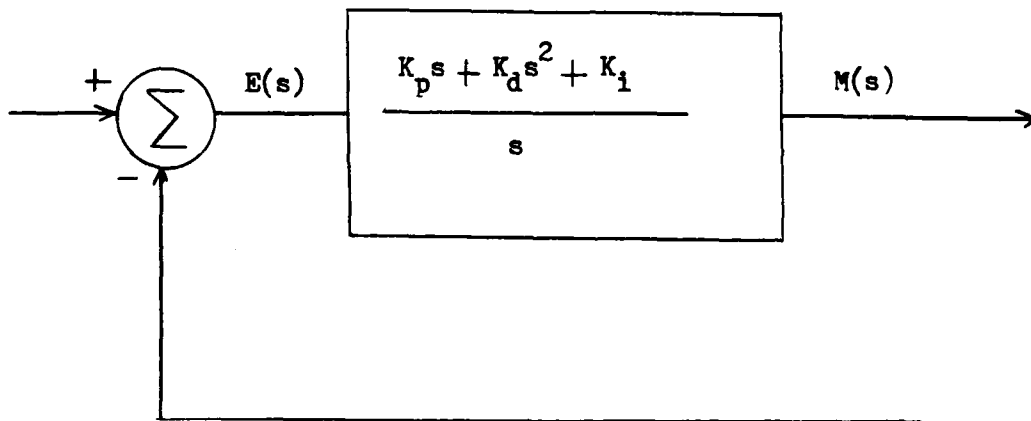


FIGURE 4-1 PID CONTROL BLOCK DIAGRAM

PID control incorporates the advantages and disadvantages of proportional, derivative, and integral control. The proportional controller basically acts as an amplifier. The

derivative control provides for an anticipatory action and hence enhances stability and reduces the tendency towards oscillation. However, the derivative control tends to amplify noise signals and may have a saturation effect on the actuators. The integral control assures a reduced steady state error and enhances steady state tracking. Integral control tends to reduce stability and can lead to an oscillatory response [12].

4.2 Development of a linear PID controller

Initially it is important to attempt to design a linear PID controller that will compensate for the motion of the base. This was accomplished by first selecting nominal values for the linearization (using program developed in Chapter 3), and then design a controller for the linearized system. The nominal values, θ_1^n selected for this particular linearization are:

$$\theta_1^n = .349 \text{ radians}$$

$$\theta_2^n = .698 \text{ radians}$$

$$\dot{\theta}_1^n = \dot{\theta}_2^n = 1 \text{ rad / sec}$$

$$\ddot{\theta}_1^n = \ddot{\theta}_2^n = 1 \text{ rad / sec}^2$$

$$\dot{y}^n = 1 \text{ ft / sec}$$

$$\ddot{y}^n = 1 \text{ ft / sec}^2$$

These nominal values are depicted in the following illustration:

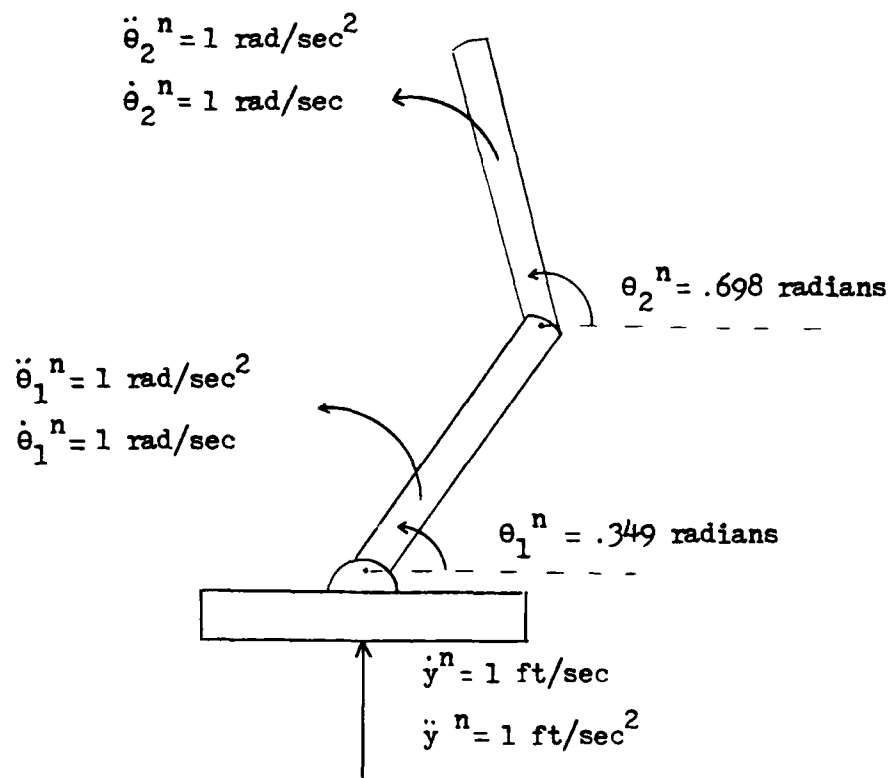


FIGURE 4-2 NOMINAL VALUES FOR LINEAR CONTROLLER

These nominal values were selected because they provide for a realistic description of system performance. The nominal joint angles provide for a realistic configuration of the manipulator during its prescribed motion, and also lead to an examination of torque capabilities. The nominal velocity and acceleration terms provide for link motion that would lead to acceptable cycle time.

Utilizing the linearization procedure developed in Chapter 3, along with the program LINEAR (Appendix B), the equations of motion (equations 3.10 and 3.11) are linearized about the selected nominal values. The linearized equations become:

$$\begin{aligned} \delta \ddot{\theta}_1 = & -11.79 \delta \theta_1 + 1.13 \delta \dot{\theta}_1 + 10.33 \delta \theta_2 + .791 \delta \dot{\theta}_2 \\ & + .099 \dot{y} - .464 \ddot{y} + .021 T_1 - .048 T_2 \end{aligned} \quad (4.2)$$

$$\begin{aligned} \delta \ddot{\theta}_2 = & 16.21 \delta \theta_1 - 2.43 \delta \dot{\theta}_1 - 21.60 \delta \theta_2 - 1.03 \delta \dot{\theta}_2 \\ & - .130 \dot{y} + .251 \ddot{y} - .028 T_1 + .089 T_2 \end{aligned} \quad (4.3)$$

These equations of motion can now be placed in state-space form. As was described in Chapter 3, the equations take the form of:

$$\dot{\underline{x}} = \underline{\bar{A}} \underline{x} + \underline{\bar{B}} \underline{u} + \underline{\bar{\Gamma}} \underline{w} \quad (4.4)$$

$$\underline{y} = \underline{\bar{C}} \underline{x} + \underline{\bar{D}} \underline{u} \quad (4.5)$$

where

$$\underline{x}^T = [x_1, x_2, x_3, x_4, x_5] \quad (4.6)$$

$$= [\delta \theta_1, \delta \dot{\theta}_1, \delta \theta_2, \delta \dot{\theta}_2, \dot{y}]$$

$$\underline{u}^T = [u_1, u_2] \quad (4.7)$$

$$= [T_1, T_2]$$

$$\underline{w} = [\ddot{y}] \quad (4.8)$$

Using this format the open loop system state equations become:

$$\frac{d}{dt} \begin{bmatrix} x_1 \\ x_2 \\ x_3 \\ x_4 \\ x_5 \end{bmatrix} = \begin{bmatrix} 0 & 1 & 0 & 0 & 0 \\ -11.79 & 1.13 & 10.33 & .791 & .099 \\ 0 & 0 & 0 & 1 & 0 \\ 16.21 & -2.43 & -21.60 & -1.03 & -.130 \\ 0 & 0 & 0 & 0 & 0 \end{bmatrix} \begin{bmatrix} x_1 \\ x_2 \\ x_3 \\ x_4 \\ x_5 \end{bmatrix} + \begin{bmatrix} 0 & 0 \\ .021 & -.048 \\ 0 & 0 \\ -.028 & .089 \\ 0 & 0 \end{bmatrix} \begin{bmatrix} T_1 \\ T_2 \end{bmatrix} + \begin{bmatrix} 0 \\ -.464 \\ 0 \\ .251 \\ 0 \end{bmatrix} [\ddot{y}] \quad (4.9)$$

$$y = \begin{bmatrix} \theta_1 \\ \theta_2 \end{bmatrix} = \begin{bmatrix} 1 & 0 & 0 & 0 & 0 \\ 0 & 0 & 1 & 0 & 0 \end{bmatrix} \underline{x} \quad (4.10)$$

Since this PID controller does not take into consideration the motion of the base (i.e. it is assumed that it receives no sensory information as to the base motion), the controller will be designed ignoring the base motion. This is accomplished by ignoring the \dot{y} and \ddot{y} terms in the equations of motion. This transforms the system matrices to:

$$\begin{aligned}\bar{A} &= \begin{bmatrix} 0 & 1 & 0 & 0 \\ -11.79 & 1.13 & 10.33 & .791 \\ 0 & 0 & 0 & 1 \\ 16.21 & -2.43 & -21.60 & -1.03 \end{bmatrix} & \bar{B} &= \begin{bmatrix} 0 & 0 \\ .021 & -.048 \\ 0 & 0 \\ -.028 & .089 \end{bmatrix} \\ & & & (4.11) \\ \bar{C} &= \begin{bmatrix} 1 & 0 & 0 & 0 \\ 0 & 0 & 1 & 0 \end{bmatrix} & D &= \begin{bmatrix} 0 & 0 \\ 0 & 0 \end{bmatrix}\end{aligned}$$

The open loop system transfer function is defined as the ratio of the Laplace transform of the output (response function, $\theta_1(s)$ and $\theta_2(s)$) to the Laplace transform of the input (driving function, $T_1(s)$ and $T_2(s)$) [12]. In this case the system transfer function becomes:

$$\bar{G}_p(s) =$$

$$\frac{\begin{vmatrix} .021 s^2 + .0189 s + .1644 & -.048 s^2 - .0406 s - .1174 \\ -.028 s^2 - .0194 s + .0103 & .089 s^2 + .0161 s + .2712 \end{vmatrix}}{s^4 - .1 s^3 + 32.4667 s^2 + 11.2328 s + 87.2147}$$

(4.12)

This transfer function can also be represented in the following manner:

$$\bar{G}_p(s) = \begin{vmatrix} g_{11} & g_{12} \\ g_{21} & g_{22} \end{vmatrix} \quad (4.13)$$

This is the open loop transfer function, i.e. the transfer function of the passive system in the absence of control. It is important to note that the linearized system itself is inherently unstable. This is evident by applying the Routh criterion to the system transfer function [12]. In addition investigation of the open loop poles of the system also indicate instability. The open loop poles of this system are:

$$\begin{aligned}
 p_1 &= .2648 + 5.4492 i \\
 p_2 &= .2648 - 5.4492 i \\
 p_3 &= -.2148 + 1.6983 i \\
 p_4 &= -.2148 - 1.6983 i
 \end{aligned}
 \tag{4.14}$$

The last two poles lie in the right half side of the complex plane and hence are unstable poles. This inherent instability is a result of including the gravitational effects in the equations of motion.

As was stated earlier, PID controllers are designed based on the concept of independent joint control, also referred to as single axis control. In other words, the motion of link one is controlled by control inputs applied to the first actuator, and the motion of link two is controlled by inputs applied to the second actuator. The coupling effect resulting from the system nonlinearities is ignored. Utilizing this approach, linear controllers for each of the two joints are

now designed.

FOR JOINT ONE

Joint one has the torque applied to the first actuator as its input and θ_1 , the angle of the first link, as its output. As is depicted in the system transfer function this relationship is described by the single input single output transfer function, g_{11} . For the design of this controller, g_{11} acts as G_p . The controller transfer function, G_c is given by the dynamics of the PID controller:

$$G_c = K_p + K_d s + K_i / s = \frac{K_p s^2 + K_d s + K_i}{s} \quad (4.15)$$

where: K_p = proportional gain

K_d = derivative gain

K_i = integral gain

The closed loop transfer function of the system is given by the relation:

$$TF_{cl} = \frac{G_c G_p}{1 + G_c G_p} \quad (4.16)$$

Linear simulations, varying the values of the constant gains, were conducted in order to design an acceptable controller. The gains to be tested were initially selected by classical control theory and then verified by simulation. The simulations were conducted by commanding the joint angles to moved to some point that was within a small perturbation from the linearized position. This is an important point. By definition, the linearized equations are only valid for some small perturbation around the selected nominal values. For the purposes of these simulations the pertubation will be no greater that 15 degrees (.26 radians). In the first simulation relatively small gains ($K_p = K_d = K_i = 100$) were chosen. A simulation was then conducted, with the following results:

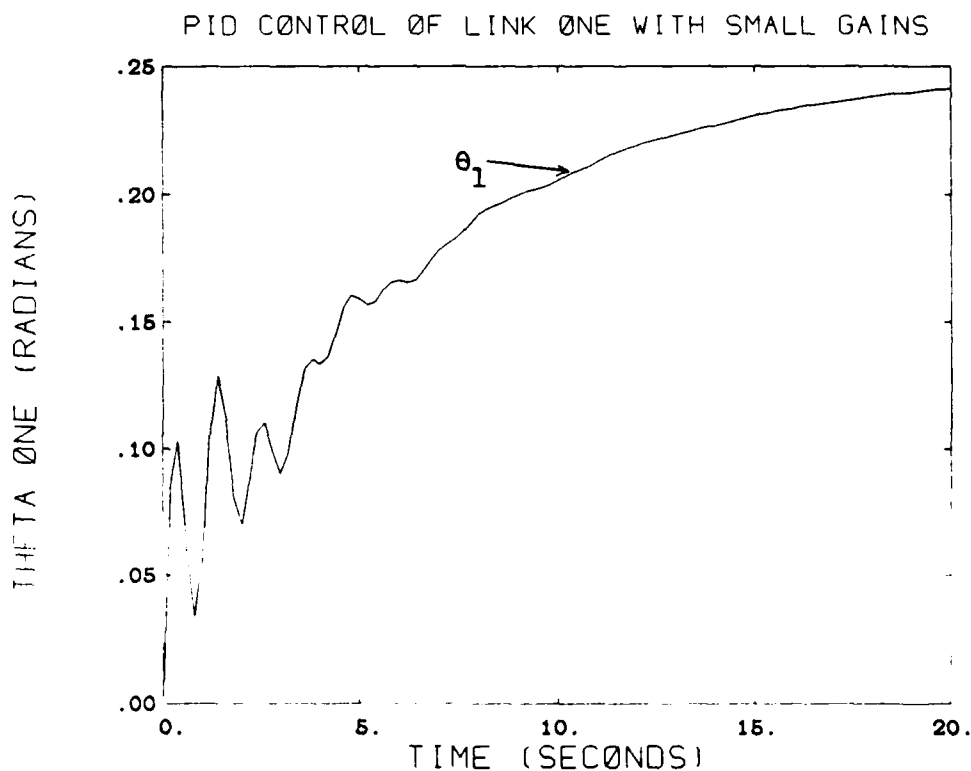


FIGURE 4-3 PID CONTROL WITH SMALL GAINS

An interpretation of these results leads to an interesting insight. By utilizing small gains the final value was eventually reached, but the response time is unacceptable. In addition, oscillations exist that are unacceptable. Increasing the gains to $K_p = K_d = K_i = 1000$ leads to the following results:

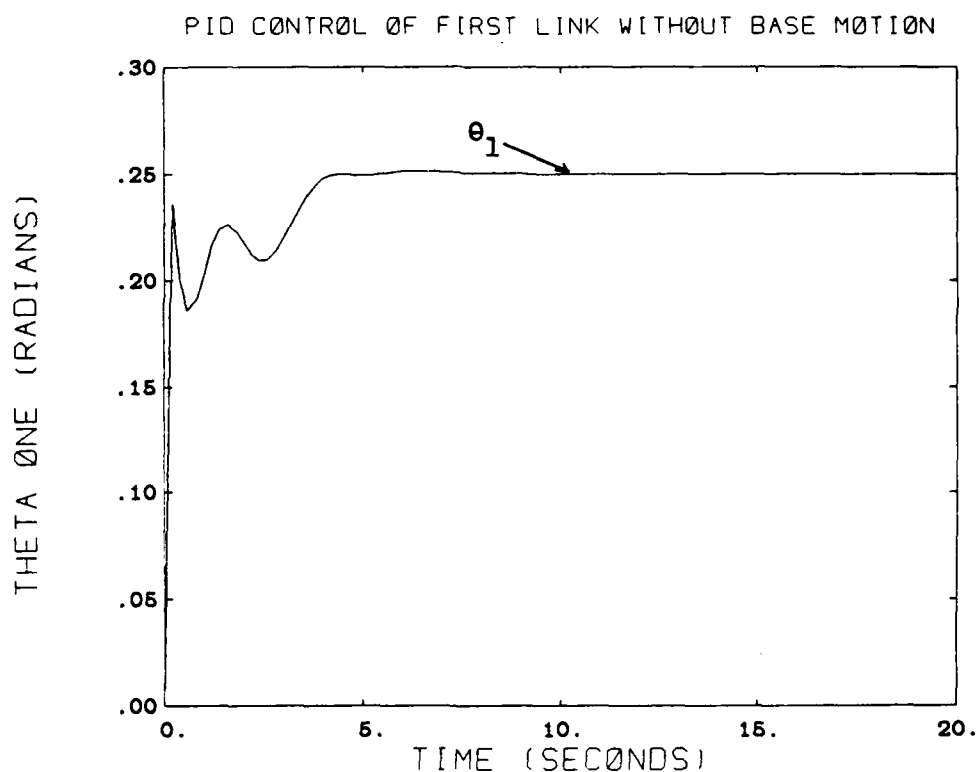


FIGURE 4-4 PID CONTROL WITH LARGER GAINS

These results are more acceptable. The response time is quicker, and less oscillations exist. It was found that by

continuing to increase the gains, better results could be obtained. However, very large gains are unrealistic in actual system implementation, primarily due to the interaction with structural resonances and control computer sampling times. In addition, with large gains actuator saturation becomes a problem.

JOINT TWO

The same design procedure was utilized in designing a controller that would be used at the second joint to control the position of the second link. In this case g_{22} becomes the system transfer function. Once again, increased gains provided for more acceptable results. Using the values of $K_p = K_d = K_i = 1000$ the following results were obtained:

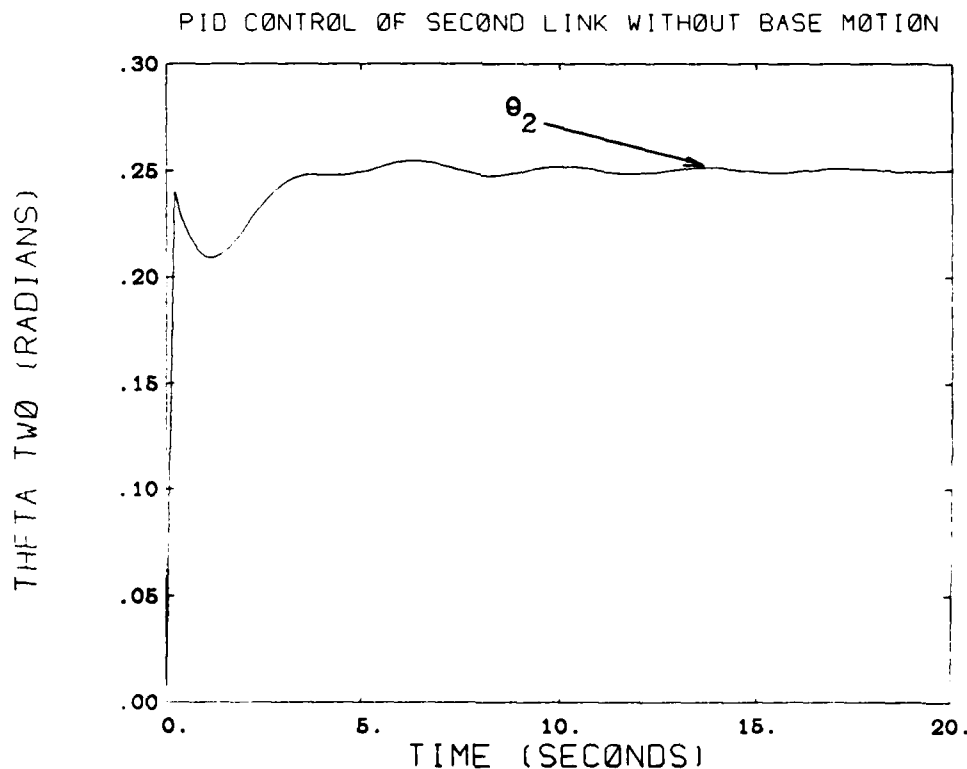


FIGURE 4-5 PID CONTROL OF LINK TWO

It is important to understand the ramifications of increasing the gains in this PID controller. As was indicated in the above simulations, increasing the gains led to faster response time. This response time, as was stated in Chapter 2, is a function of the bandwidth of the controller. For illustration purposes, the bandwidth of the two controllers simulated (i.e. when $K_i = 100$ and when $K_i = 1000$) were determined. These bandwidths are as evidenced in the following closed loop Bode plots:

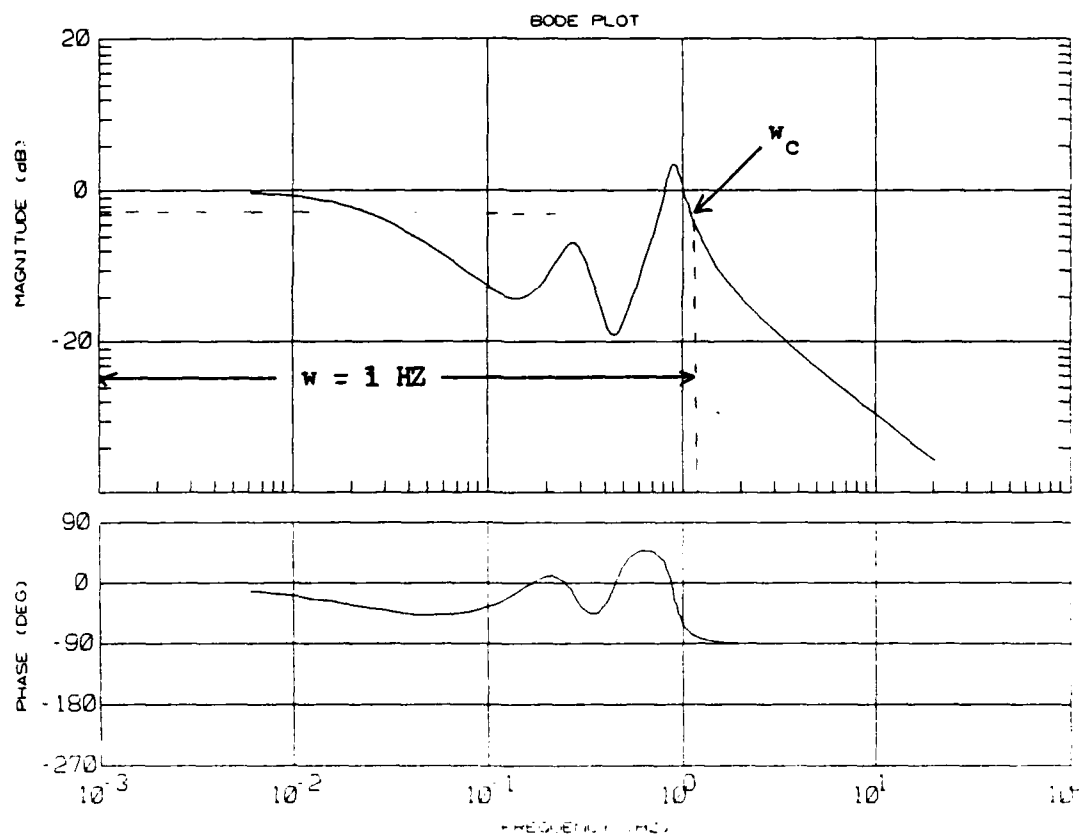


FIGURE 4-6 BODE PLOT OF PID CONTROLLER WITH SMALL GAINS

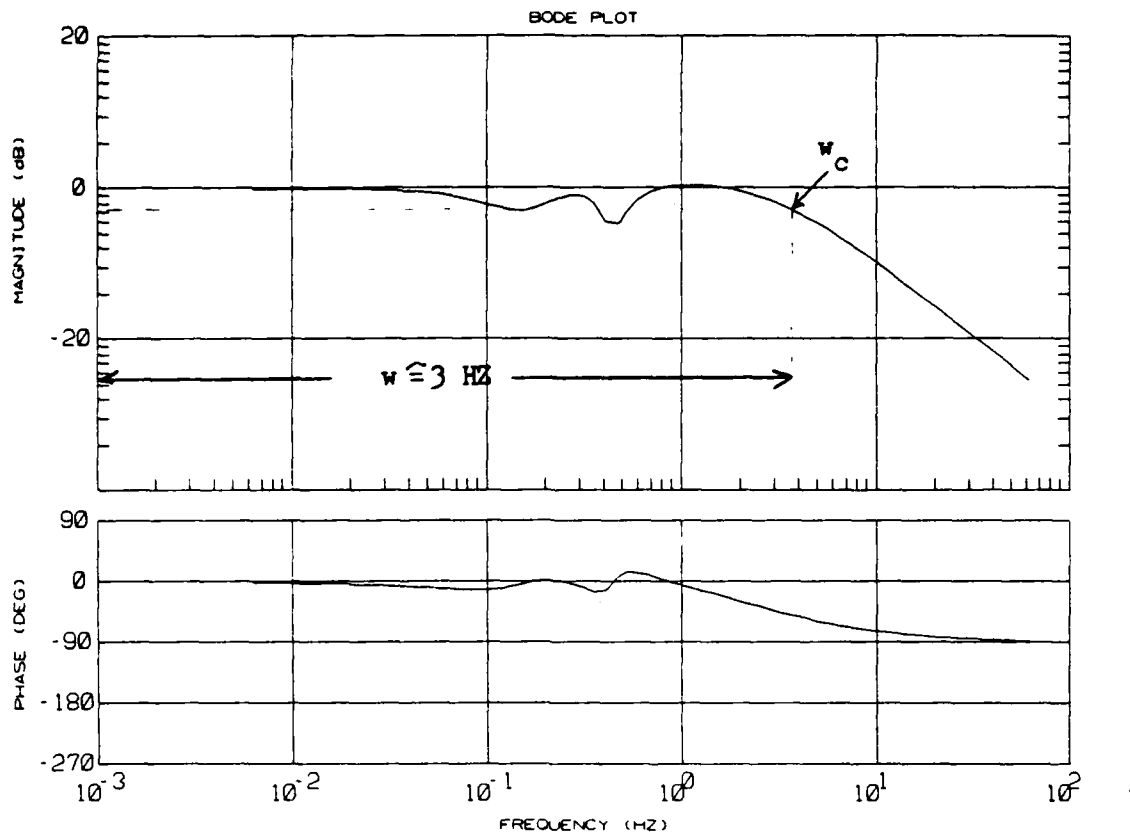


FIGURE 4-7 BODE PLOT FOR PID CONTROLLER WITH LARGER GAINS

The bandwidth is determined by the range of frequencies:

$$0 \leq \omega \leq \omega_c \quad (4.17)$$

where ω_c is the frequency at which the magnitude of the closed loop frequency response is 3 db below its zero frequency value [12].

An interpretation of this result is that the bandwidth of the controller with large gains is greater than that of the controller designed with small gains.

In order for a system to follow arbitrary inputs accurately, the system must have a large bandwidth. In essence, the bandwidth of the controller must be larger than the bandwidth of any inputs that it is designed to compensate for. The problem lies in the fact that increase bandwidth is a result of higher gains which could result in such problems as actuator saturation, excessive noise, etc.

It is important to reemphasize the fact that PID control is based on the concept of individual joint control. The coupling dynamics of the system are ignored. In actual system implementation, the dynamics of the actuators themselves (i.e. motor inertia, friction, etc.) tend to reduce the coupling dynamics and allow the PID controller to work better. Due to the fact that the model used in these simulations did not contain any of actuator dynamics, a simulation of the entire system under PID control did not lead to acceptable results.

Once again disregarding the coupling dynamics, the manipulator under independent joint PID control is subject to base motion in order to see whether or not the PID controller could compensate for the motion of the base. Focusing on the controller designed for the first actuator and the first link, the manipulator is now subjected to base velocity and accelerations of the magnitude described in preceeding chapters. A linear simulation was conducted, with the following results:

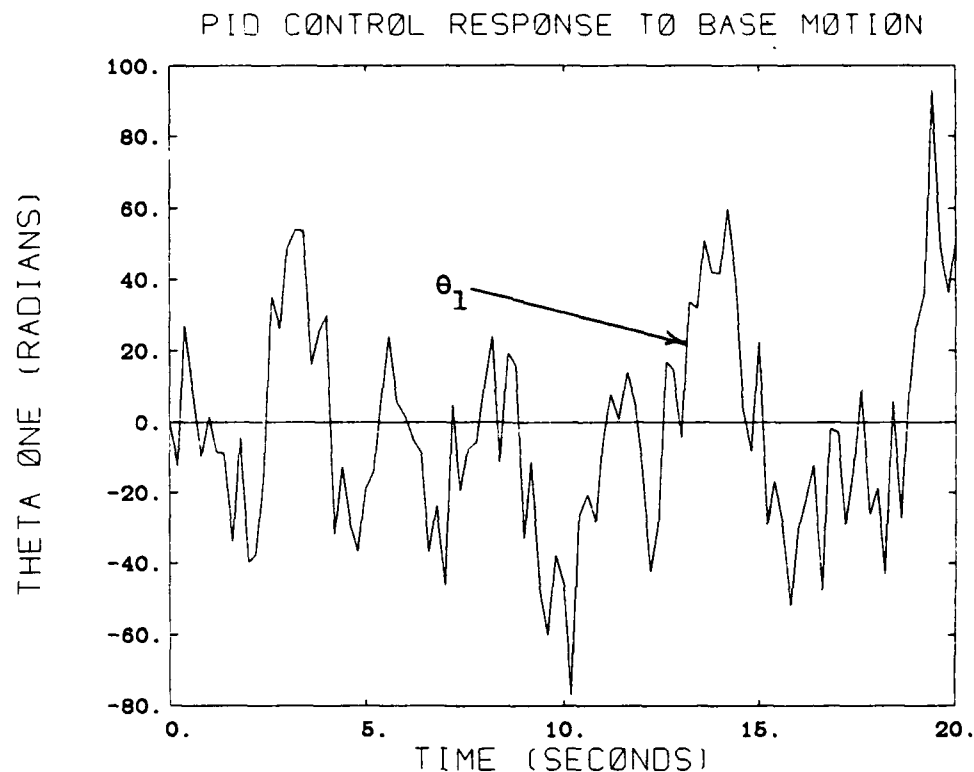


FIGURE 4-8 PID CONTROL RESPONSE TO BASE DISTURBANCE

Clearly, the PID controller is unable to compensate for the base motion. The random base acceleration led to wild oscillations of the link, and a steady state value was not obtained. It must be remembered that this simulation was conducted in the most simple region, totally ignoring the coupling effects of the dynamics of the manipulator and also ignoring all nonlinear effects. As was stated in Chapter 2, the bandwidth of the base acceleration is extremely high. The PID controller bandwidth was less than that of the disturbance, and hence the controller was not able to

compensate for the motion of the base. It is possible that the controller bandwidth could be increased to the point where it was larger than the bandwidth of the disturbance, but this would not be practical with actual system components. The actuators would have to be very strong to accept such large gains, and would therefore be extremely expensive and bulky.

4.3 Summary

It was shown in this chapter that conventional control strategies are not appropriate for a manipulator mounted on a moving base. Due to the extremely high bandwidth of the disturbance, a realistic PID controller could not be designed with a bandwidth high enough to compensate for the motion of the base. Actuator saturation, along with additional problems such as noise and structural resonance frequency interference, limit the realistic gains that can be applied to a PID controller.

CHAPTER 5

ADVANCED CONTROL STRATEGIES

5.1 Discussion of advanced control strategies

It was illustrated in the preceeding chapter that conventional control algorithms were not effective in the moving base problem. PID control was unable to effectively compensate for the motion of the base. This chapter will be devoted to applying more advanced linear control strategies to the moving base problem in an attempt to see if they prove to be more effective in dealing with the moving base. First, decoupling control will be investigated [13]. This is primarily a control algorithm that eliminates the coupling dynamics of the manipulator. The results of this portion will be particularly interesting based on the high degree of coupling in the robotic manipulator. Secondly, Linear Quadratic Regulator Theory (LQR) will be applied to the moving base problem [9]. LQR control is a state variable feedback technique which attempts to arrive at an optimal control strategy. Finally, a pole placement technique will be examined. This technique attempts to achieve stability and desired response by adjusting the location of the system's closed loop eigenvalues. It is important to note that these control strategies are all based on an assumption of linearity within the system. All controllers designed in this chapter, along with all simulations conducted, will be in the linear mode.

5.2 Decoupling control

Decoupling control is a matrix manipulation technique that allows for diagonalizing the system transfer function, $G(s)$ [13]. It is based on the following development:

Given the state-space description in the form of:

$$\dot{\underline{x}} = \underline{\bar{A}} \underline{x} + \underline{\bar{B}} \underline{u} \quad (5.1)$$

$$\underline{y} = \underline{\bar{C}} \underline{x} \quad (5.2)$$

$$\text{let } \underline{r}(t) = \text{reference signal} \quad (5.3)$$

and the control input

$$\underline{u} = -\underline{\bar{K}}_d \underline{x} + \underline{\bar{T}}_d \underline{r}(t) \quad (5.4)$$

Substituting equation 5.4 into equation 5.1 leads to

$$\dot{\underline{x}} = (\underline{\bar{A}} - \underline{\bar{B}} \underline{\bar{K}}_d) \underline{x} + \underline{\bar{B}} \underline{\bar{T}}_d \underline{r}(t) \quad (5.5)$$

which implies that:

Defining

$$\underline{\bar{A}'} = \underline{\bar{A}} - \underline{\bar{B}} \underline{\bar{K}}_d \quad (5.6)$$

$$\underline{\bar{B}'} = \underline{\bar{B}} \underline{\bar{T}}_d \quad (5.7)$$

The closed loop system transfer function in the Laplace domain is defined as the ratio of the output to the input which in this case [9]:

$$\bar{G}(s) = \frac{y(s)}{r(s)} = \bar{C} (s \bar{I} - \bar{A})^{-1} \bar{B} \quad (5.8)$$

substituting in the values for \bar{A}' and \bar{B}' from equations 5.6 and 5.7 into equation 5.8 leads to:

$$\bar{G}(s) = \bar{C} (s \bar{I} - \bar{A} + \bar{B} \bar{K}_d^{-1} \bar{B} \bar{T}_d) \quad (5.9)$$

In order to have perfect decoupling $G(s)$ must be a diagonal matrix (i.e. all zeros on any off-diagonal element)[9]. Based on equation 5.9 in order for $G(s)$ to be diagonal,

$$\bar{C} (\bar{A} - \bar{B} \bar{K}_d^{-1} \bar{B} \bar{T}_d) \text{ for } j=0, \dots, n-1 \quad (5.10)$$

must also be diagonal.

This can be accomplished only by proper selection of \bar{K}_d and \bar{T}_d . Selection of \bar{K}_d and \bar{T}_d accomplished in the following manner:

$$\text{Define the integers } d_i = \min \{j | \bar{C} \bar{A}^j \bar{B} = 0, j=0, \dots, n-1\} \quad (5.11)$$

$$\text{let } \bar{N} = \begin{bmatrix} C A^{d_1} B \\ 1 \\ \vdots \\ C A^{d_m} B \\ m \end{bmatrix} \quad (5.12)$$

m x m

The system can be decoupled only if \bar{N} is non singular.

The following matrices will then decouple the system:

$$\bar{T}_d = \bar{N}^{-1} \quad \bar{K}_d = \bar{N}^{-1} \begin{bmatrix} C A^{d_i+1} \\ \vdots \\ C A^{d_i+1} \end{bmatrix} \quad (5.13)$$

The following block diagram illustrates the decoupling control technique:

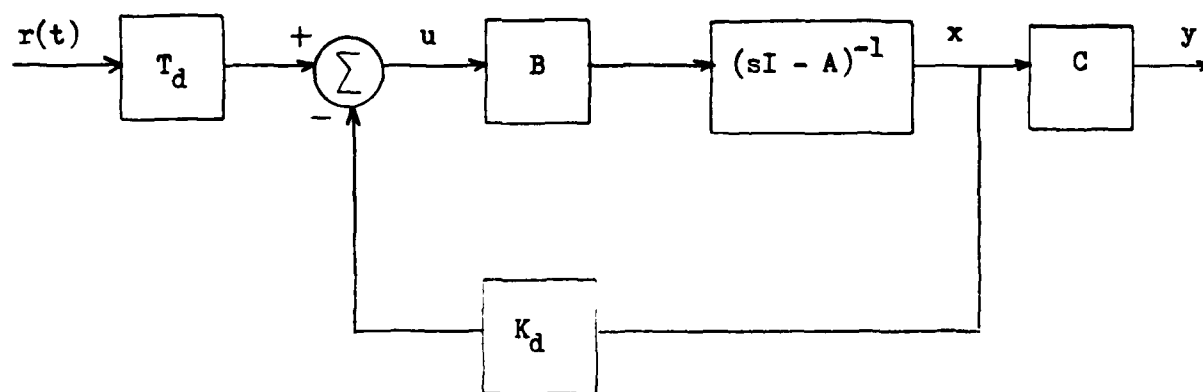


FIGURE 5-1 DECOUPLING CONTROL BLOCK DIAGRAM

Once the system has been decoupled, the system can be controlled by either placing a single input, single output controller around each loop.

The above procedure is now applied to the equations of motion for the system linearized about the nominal values that were used for designing the PID controller. Designing the controller in the absence of base motion using the open loop linearized system matrices:

$$\bar{A} = \begin{bmatrix} 0 & 1 & 0 & 0 \\ -11.79 & 1.13 & 10.33 & .791 \\ 0 & 0 & 0 & 1 \\ 16.21 & -2.43 & -21.60 & -1.03 \end{bmatrix}$$

$$\bar{B} = \begin{bmatrix} 0 & 0 \\ .021 & -.048 \\ 0 & 0 \\ -.028 & .089 \end{bmatrix}$$

(5.14)

$$\bar{C} = \begin{bmatrix} 1 & 0 & 0 & 0 \\ 0 & 0 & 1 & 0 \end{bmatrix}$$

$$\bar{D} = \begin{bmatrix} 0 & 0 \\ 0 & 0 \end{bmatrix}$$

Utilizing the previous technique leads to:

$$\begin{bmatrix} C & A^0 & B \end{bmatrix}_1 = \begin{bmatrix} 0 & 0 \end{bmatrix}$$

$$\begin{bmatrix} C & A^1 & B \end{bmatrix}_1 = \begin{bmatrix} .021 & -.048 \end{bmatrix} \text{ implies that } d_1 = 1$$

(5.15)

$$\begin{bmatrix} C & A^0 & B \end{bmatrix}_2 = \begin{bmatrix} 0 & 0 \end{bmatrix}$$

$$\begin{bmatrix} C & A^1 & B \end{bmatrix}_2 = \begin{bmatrix} -.028 & -.089 \end{bmatrix} \text{ implies that } d_2 = 1$$

which leads to:

$$\bar{N} = \begin{vmatrix} C^1 & A^1 & B \\ C_1 & A^1 & B \\ C_2 & A^1 & B \end{vmatrix} = \begin{bmatrix} .021 & -.048 \\ -.028 & .089 \end{bmatrix} \quad (5.16)$$

$$\bar{T}_d = \bar{N}^{-1} = \begin{vmatrix} 169.5238 & 91.4286 \\ 53.3333 & 40.0000 \end{vmatrix} \quad (5.17)$$

$$\bar{K}_d = \begin{vmatrix} C^2 & A^2 \\ C_1 & A^2 \\ C_2 & A^2 \end{vmatrix} \quad (5.18)$$

$$= \begin{vmatrix} -516.6286 & -30.6095 & -223.6762 & 39.9219 \\ 19.6000 & -36.9333 & -313.0667 & .9867 \end{vmatrix}$$

$$\bar{A}' = \bar{A} - \bar{B} \bar{K}_d = \begin{vmatrix} 0 & 1 & 0 & 0 \\ 0 & 0 & 0 & 0 \\ 0 & 0 & 0 & 1 \\ 0 & 0 & 0 & 0 \end{vmatrix} \quad (5.19)$$

$$\bar{B}' = \bar{B} \bar{T}_d = \begin{vmatrix} 0 & 0 \\ 1 & 0 \\ 0 & 0 \\ 0 & 1 \end{vmatrix} \quad (5.20)$$

The decoupled system transfer function becomes:

$$\bar{G}_p(s) = \begin{vmatrix} g_{11} & g_{12} \\ g_{21} & g_{22} \end{vmatrix} \quad (5.21)$$

$$\frac{\bar{G}}{p}(s) = \frac{\begin{vmatrix} s^2 & 0 \\ 0 & s^2 \end{vmatrix}}{s^4}$$

The task is now to design an SISO controller for each of the single axis control loops. It was found that an acceptable controller proved to be a compensator of the form:

$$G_c(s) = \frac{10(s + .1)}{s + 2} \quad (5.22)$$

The closed loop system transfer function then becomes:

$$TF_{cl} = \frac{G_c g_{ll}}{1 + G_c g_{ll}} = \frac{10s + 1}{s^3 + 2s^2 + 10s + 1} \quad (5.23)$$

A simulation was then conducted to test the performance of this SISO controller. Again, concentrating on small

perturbations from the linearized positions, the following results were obtained:

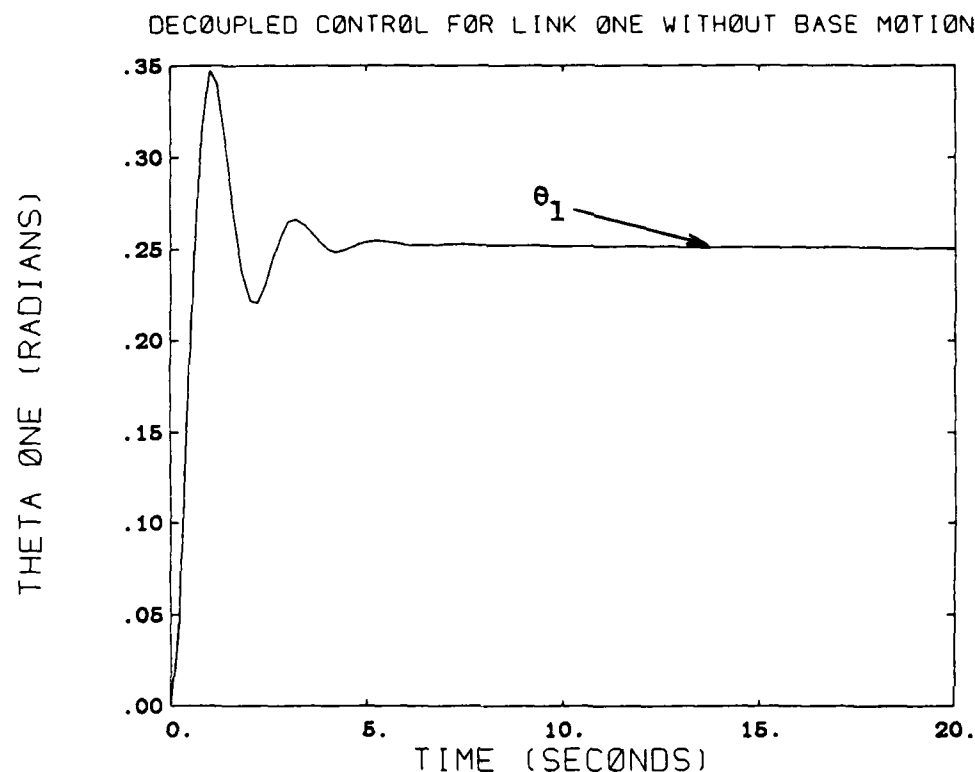


FIGURE 5-2 DECOUPLED CONTROL FOR LINK ONE

These results are acceptable, given the specifications outlined in Chapter 2. The response time is within 5 seconds, and stability and accuracy are achieved. Based on the dynamics of the decoupled system, the controller for the second control loop would be the same. A linear simulation was now conducted for the entire system to check response. The system has been linearized about the nominal values described for the PID controller, and the joint angles were commanded to go to values within a small perturbation from

their linearized positions. The results are:

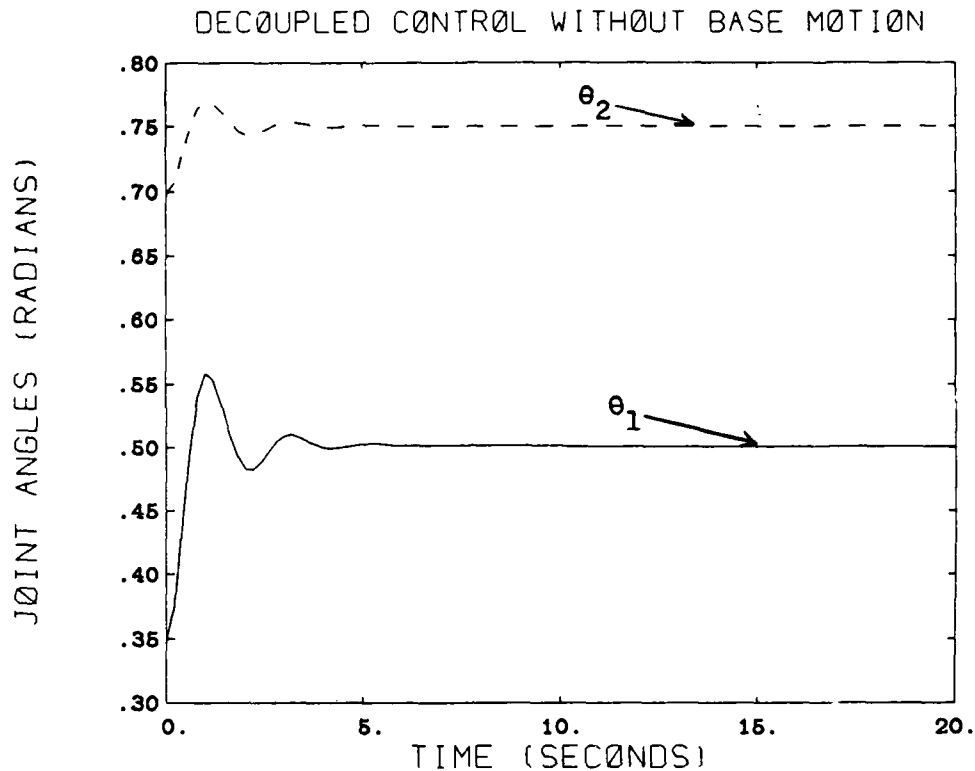


FIGURE 5-3 SYSTEM DECOUPLING CONTROL

These results for the system meet the specifications outlined for a desirable controller. The end effector location is within allowable tolerances, and the response time is acceptable. The coupling dynamics of the system have been damped, and the system has been successfully decoupled.

The problem now is to subject this controller to the dynamics of the moving base to determine whether or not it can compensate for the base motion. A simulation was conducted in which the system was augmented to account for the motion of the base. This was accomplished by adding the base motion

terms (\dot{y} and \ddot{y}) back into the equations of motion. The augmented system was then disturbed by a base acceleration of the magnitude described in Chapter 2. The following results were obtained:

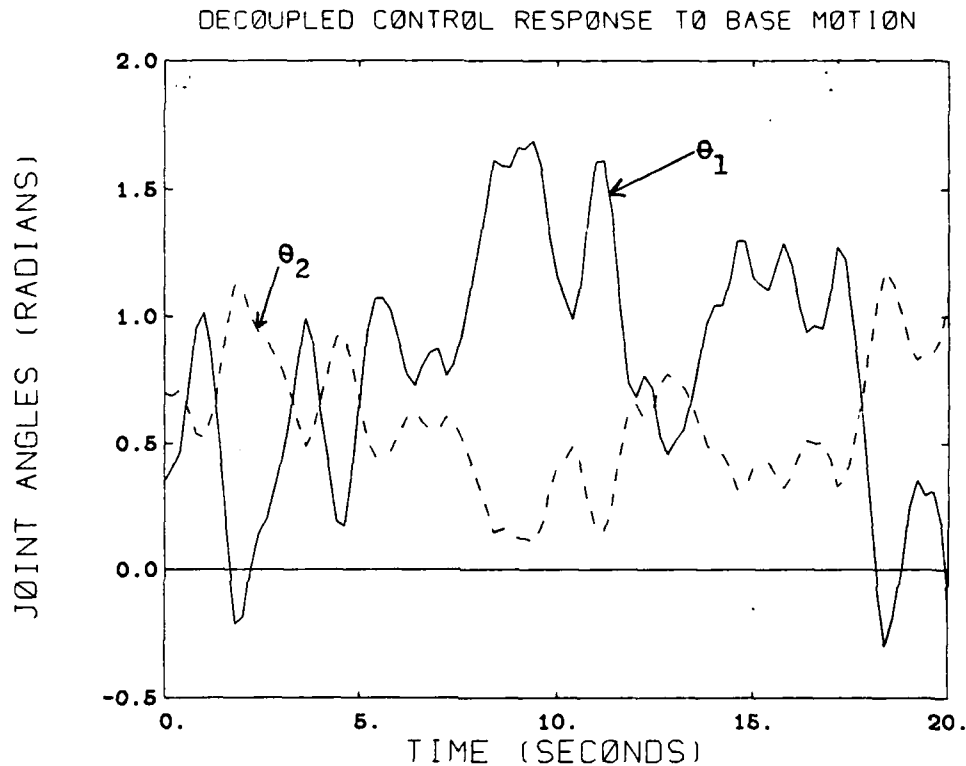


FIGURE 5-4 DECOUPLED CONTROL RESPONSE TO BASE MOTION

These results are obviously not acceptable. The base motion created large oscillations in the system performance, and stability was not achieved after twenty seconds. Although decoupling control effectively resolved the problem of the high degree of coupling between the two links, it was not able to compensate for the large base disturbances. It was found that the decoupled system was robust enough to accomodate

small disturbances, but not those of the magnitude under investigation here. The problem again, as with the PID controller, lies in the fact that the bandwidth of the controller is smaller than the bandwidth of the disturbance. The poles of the closed loop system under decoupled control are as indicated below:

$$p_1 = -.949 + 2.9843 i$$

$$p_2 = -.949 - 2.9843 i$$

$$p_3 = -.949 + 2.9843 i$$

$$p_4 = -.949 - 2.9843 i$$

Investigation of the closed loop pole locations indicate that the system bandwidth is now of the order of 3 hertz. This is smaller than the bandwidth of the disturbance, and hence it is not able to compensate for the disturbance. However, increasing the bandwidth again leads to increased gains and possible actuator saturation.

5.3 Linear Quadratic Regulator (LQR) Control

The next step in the investigation was to design a controller utilizing linear quadratic regulator theory, in an attempt to see how that particular control design does in regards to the base acceleration.

LQR theory is a state variable feedback technique that assumes full state feedback, i.e. all states must be available for measurement [9]. The basic premise involves choosing the control vector $u(t)$ such that a particular performance index, J , is minimized. J is given by the equation:

$$J = \int_0^T \underline{x}^T(t) S_f \underline{x}(t) + 1/2 (\underline{x}^T \underline{Q} \underline{x} + \underline{u}^T \underline{R} \underline{u}) dt \quad (5.24)$$

where: S_f is the solution to the associated matrix Ricatti equation and \underline{Q} is a positive semi-definite weighting matrix on state errors and \underline{R} is a positive definite weighting matrix on the control effort [32]. The control law that minimizes the performance index J is the simple:

$$\underline{u} = -\underline{K} \underline{x} \quad (5.25)$$

where \underline{K} is the time varying feedback matrix given by

$$\underline{K}(t) = \underline{R}^{-1} \underline{B}^T S(t) \quad (5.26)$$

It must be noted that this procedure can be used only if $[\underline{A}, \underline{C}]$ form a detectable pair, and $[\underline{A}, \underline{B}]$ form a stabilizable pair. A detectable pair is from a system in which any unobservable mode is stable. A stabilizable pair implies that any uncontrollable mode within the system is stable. This control law is considered optimal in the sense that it minimize the control effort required to keep the mean-square deviation of the states from the reference value as small as possible.

The LQR control is highly dependant upon the selection of the performance index and the weighting matrices. Design of a desireable controller becomes an iterative technique. Initial choices for the \bar{Q} and \bar{R} matrices can be made using "Bryson's Rule", which provides estimates of the weighting matrices so as to limit the state deviation and the control deflection to some desired values [16]. Bryson's rule provides for:

$$\bar{Q}_i = \frac{1}{(y_i \text{ max})^2} \quad (5.27)$$

where y_i is the maximum desired value of the output and

$$\bar{R}_i = \frac{1}{(u_i \text{ max})^2} \quad (5.28)$$

where u_i is the maximum desired value of the control.

As the values for \bar{Q} increase, the gains increase which leads to a larger bandwidth and faster response with better precision. However, this also leads to possible actuator saturations. Varying the values for \bar{R} has just the opposite effect.

Applying the theory to the investigation at hand, the first task is to select appropriate weighting matrices. Utilizing Bryson's rule leads to:

let $y_1 \text{ max} = \theta_1 \text{ max} = 2.36 \text{ radians}$

$$\begin{matrix} y \\ 2 \end{matrix} \max = \theta \begin{matrix} \max \\ 2 \end{matrix} = 3.14 \text{ radians} \quad (5.29)$$

$$\begin{matrix} u \\ 1 \end{matrix} \max = T \begin{matrix} \max \\ 1 \end{matrix} = 20 \text{ ft-lbs}$$

$$\begin{matrix} u \\ 2 \end{matrix} \max = T \begin{matrix} \max \\ 2 \end{matrix} = 20 \text{ ft-lbs}$$

These maximum values were selected based on knowledge of the system's operation and actuator constraints. These values lead to:

$$\bar{Q} = \begin{vmatrix} .180 & 0 & 0 & 0 \\ 0 & 0 & 0 & 0 \\ 0 & 0 & .101 & 0 \\ 0 & 0 & 0 & 0 \end{vmatrix} \quad (5.30)$$

$$\bar{R} = \begin{vmatrix} .0025 & 0 \\ 0 & .0025 \end{vmatrix} \quad (5.31)$$

$$\bar{K} = \bar{R}^{-1} \bar{B}^T S(t) \quad (5.32)$$

$$= \begin{vmatrix} -.0332 & 2.6244 & 1.5137 & -2.4037 \\ -2.5464 & -6.7067 & -1.0223 & 7.1092 \end{vmatrix}$$

The closed loop equation becomes:

$$\dot{\underline{x}} = (\underline{\bar{A}} - \underline{\bar{B}} \underline{\bar{K}}) \underline{x} \quad (5.33)$$

A linear simulation of the closed loop system is now

conducted. As with the previous simulations, the joint angles are commanded to go to positions that are within small perturbations of their linearized positions. The following results were obtained:

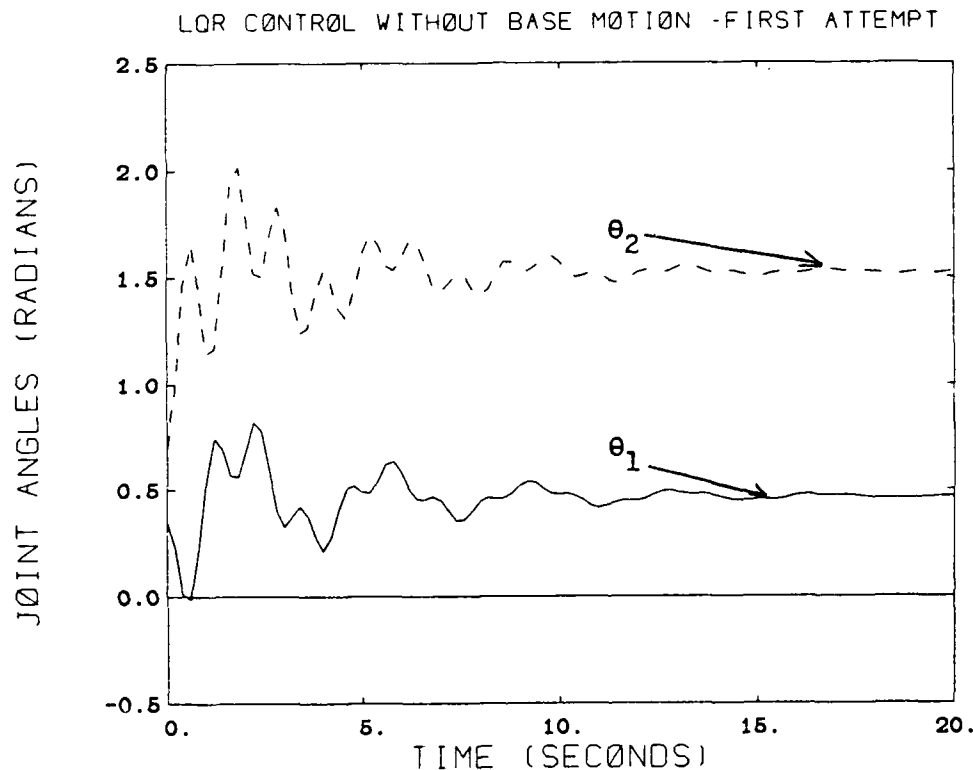


FIGURE 5-5 LQR CONTROL FIRST ATTEMPT

The LQR control theory does guarantee stability if $[A,B]$ is stabilizable, but these particular results are not acceptable. The speed of response is much too long, and too many wild oscillations exist. Since this is an iterative process, the procedure is to now vary \bar{Q} and \bar{R} until acceptable response is achieved. It was found that when:

$$\bar{Q} = \begin{bmatrix} 1000 & 0 & 0 & 0 \\ 0 & 1000 & 0 & 0 \\ 0 & 0 & 1000 & 0 \\ 0 & 0 & 0 & 1000 \end{bmatrix} \quad \bar{R} = \begin{bmatrix} .0025 & 0 \\ 0 & .0025 \end{bmatrix} \quad (5.34)$$

$$\bar{K} = \begin{bmatrix} 291.43 & 655.57 & 15.54 & 124.02 \\ -100.13 & -176.87 & 387.52 & 596.97 \end{bmatrix} \quad (5.35)$$

the response was as indicated below:

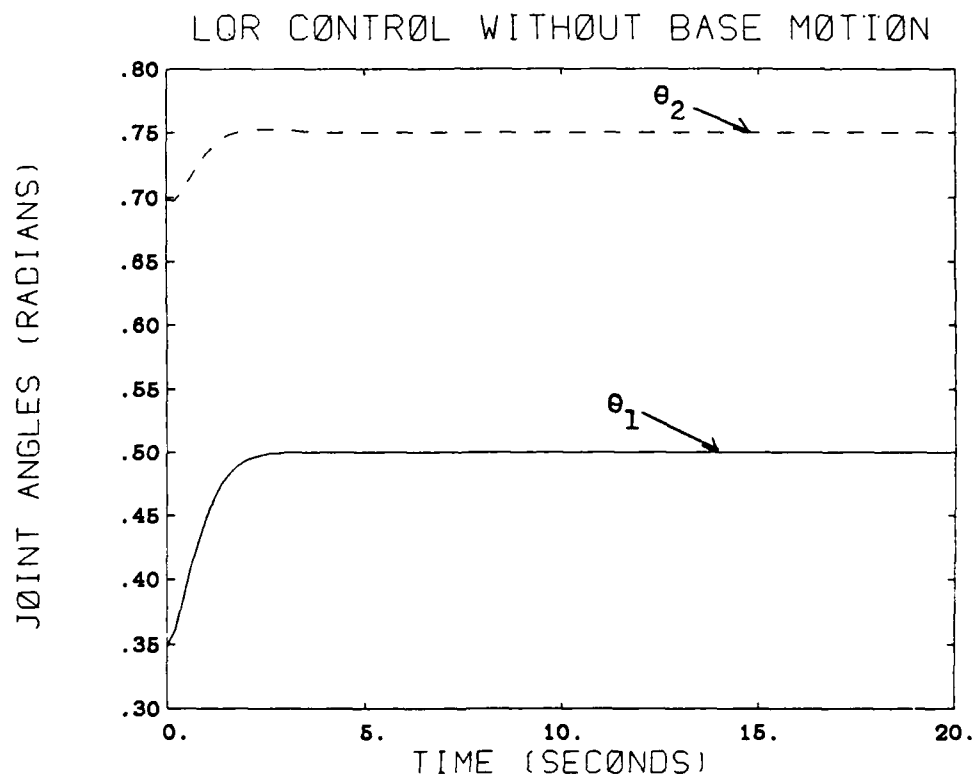


FIGURE 5-6 LQR CONTROL WITHOUT BASE MOTION

This is acceptable for the purposes of this investigation, based on the specifications outlined in Chapter 2. Now the task again becomes to subject this controller to the base accelerations of appropriate magnitude. The results of the

simulation are as indicated below:

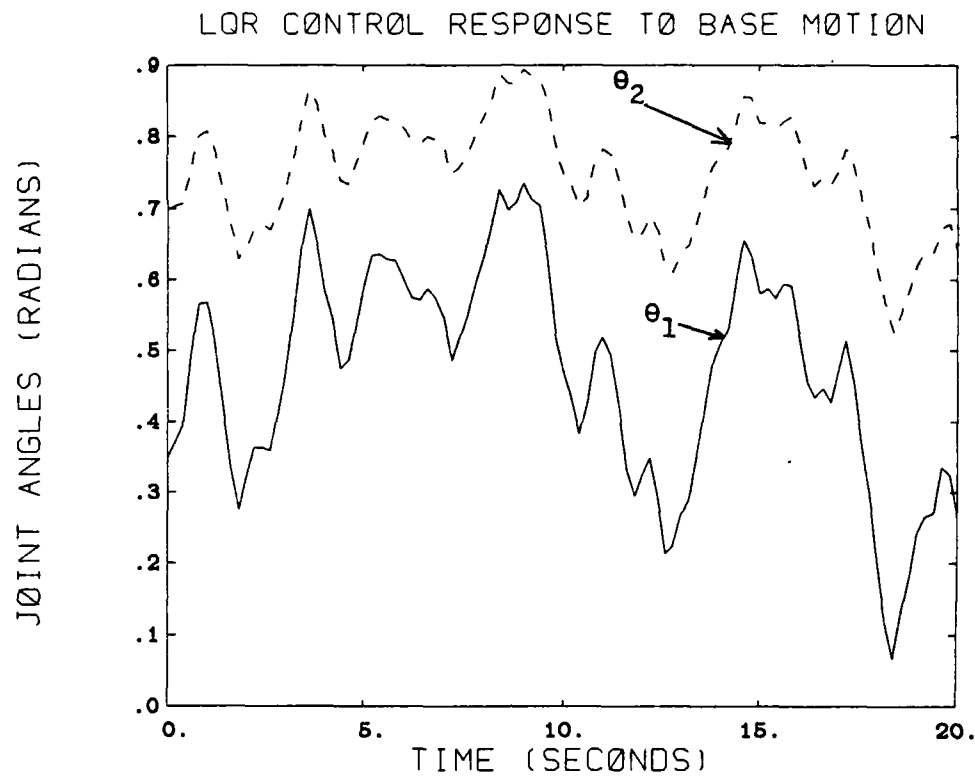


FIGURE 5-7 LQR CONTROL RESPONSE TO BASE MOTION

Obviously the controller was not able to compensate for the motion of the base. Stability was never achieved, and wild oscillations are predominant. Again the problem is bandwidth. The poles for the closed loop system under LQR control are located at:

$$p_1, p_2 = -1.78 + 1.0226 i$$

1 2

$$p_3 = -67.15 \quad p_4 = -1.1051$$

3

4

These poles indicate a system bandwidth of the order of 1.1 hertz, again too low for the bandwidth of the disturbance. Increase gains again lead to increased system bandwidth, along with the problems of actuator saturation, etc.

5.4 Pole placement technique

Another possible approach to be used in controlling a manipulator mounted on a moving base is to use a pole placement technique [10]. It is known that it is possible to place the closed loop eigenvalues (poles) of a system if the system matrices \bar{A} and \bar{B} form a controllable pair. In the full state feedback realm, gains are used to place the poles. The question becomes where to best place the poles to achieve acceptable response (see figure 5-8).

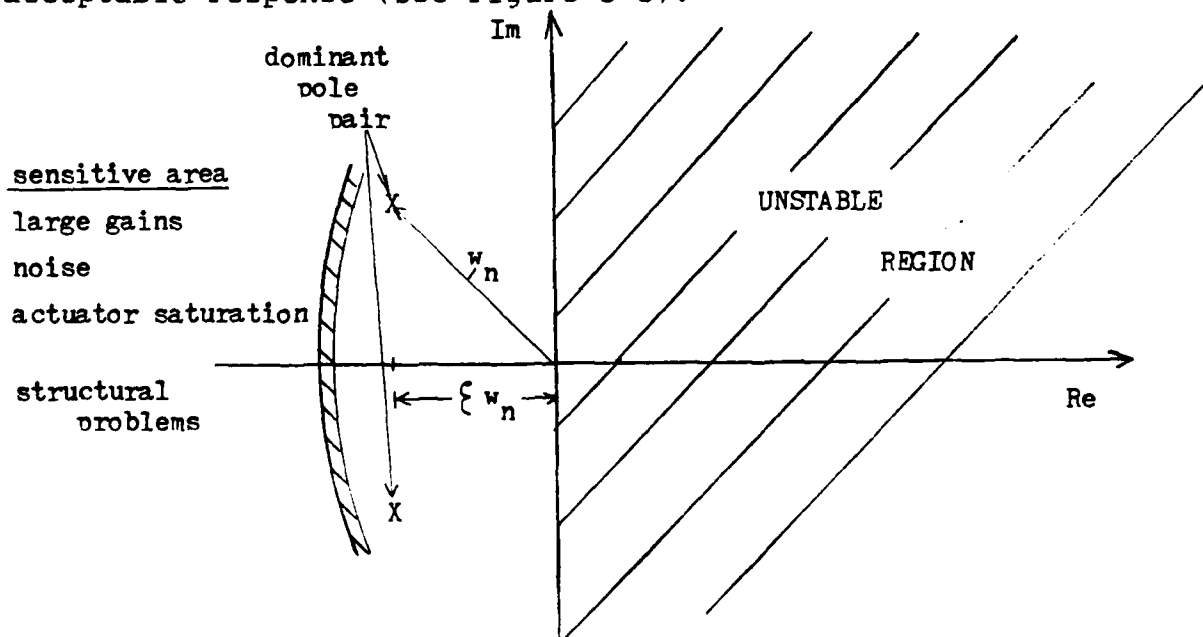


FIGURE 5-8 POSSIBLE POLE LOCATIONS

In the case of this investigation stability is a key issue, but stability obtained at the least possible cost (i.e. small gains). In addition a fast speed of response is desirable, preferably with small overshoot. The poles, for the sake of stability, must all lie in the left half plane. In addition, the farther left the poles are the more stable the system. However large gains are required to place the poles far to the left and this also leads to problems such as those associated with noise, actuator saturation, unmodeled structural dynamics and computer sampling time. The best approach is placing the poles is to use the concept of the dominant pole pair. The dominant pole pair is that pair of poles closest to the imaginary axis. This set of poles models an ideal second order system with desired speed of response. The rest of the poles are then placed far enough away as to not interfere with the dominant pole pair, but not so far as to create the problems mentioned above. The control law then becomes:

$$\underline{u} = -\underline{\bar{K}} \underline{x} \quad (5.36)$$

where $\underline{\bar{K}}$ is the matrix of gains used to place the poles.

In applying this technique to the investigation at hand it is first important to select the desired pole locations. It is important to first study the location of the open loop poles. The open loop pole locations are as indicated below:

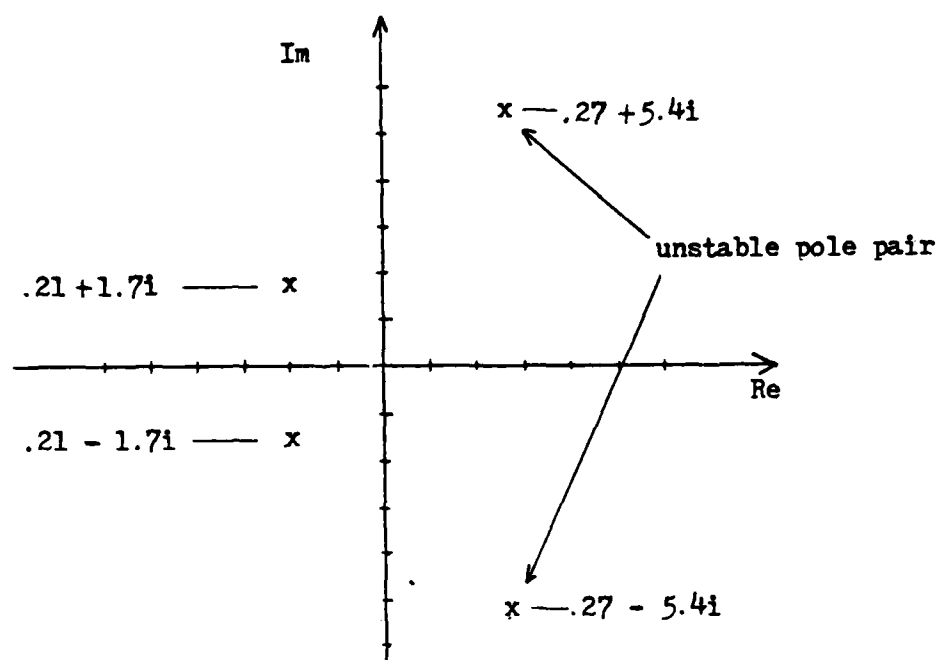


FIGURE 5-9 OPEN LOOP POLE LOCATIONS

It is important to remember that in order to achieve stability at the least cost, only those poles that need to be moved should be moved, and the poles should be placed in a location so as to receive desired response with minimal gains. This becomes an iterative procedure. Initially the poles were placed at the following locations:

$$\begin{aligned}
 p_1 &= -3.0 + 3.0 i \\
 p_2 &= -3.0 - 3.0 i \\
 p_3 &= -10.0 + 10.0 i \\
 p_4 &= -10.0 - 10.0 i
 \end{aligned}
 \tag{5.37}$$

These pole locations were chosen for the following reasons:

(1) They were all located in the left half plane which guaranteed a stable response.

(2) They provided for an optimal damping ratio of .707 which minimized overshoot.

(3) Poles 3 and 4 were placed far enough to the left so as not to interfere with the dominant pole pair, but not so far as to create extremely large gains and possible saturation problems.

The problem then became how to calculate the gains necessary to place the poles in the desired locations. A packaged program POLESYS3 [14] was used to calculate the minimum gains required to place the poles. (see Appendix C). The required gains for this particular iteration became:

$$\bar{K} = \begin{bmatrix} 1988.4 & 987.43 & 541.43 & 235.98 \\ -576.45 & -90.529 & 2242.2 & 85.686 \end{bmatrix} \quad (5.38)$$

A linear simulation of the new system was then conducted, based on the following criteria:

$$\bar{A}' = \bar{A} - \bar{B} \bar{K} \quad \underline{u} = -\bar{K} \underline{x} \quad (5.39)$$

$$\begin{aligned} \text{initial conditions: } \theta_1 &= .349 \text{ radians} \\ \theta_2 &= .698 \text{ radians} \end{aligned} \quad (5.40)$$

The system was then subjected to an input that resulted in a small perturbation from the nominal conditions, with the following results:

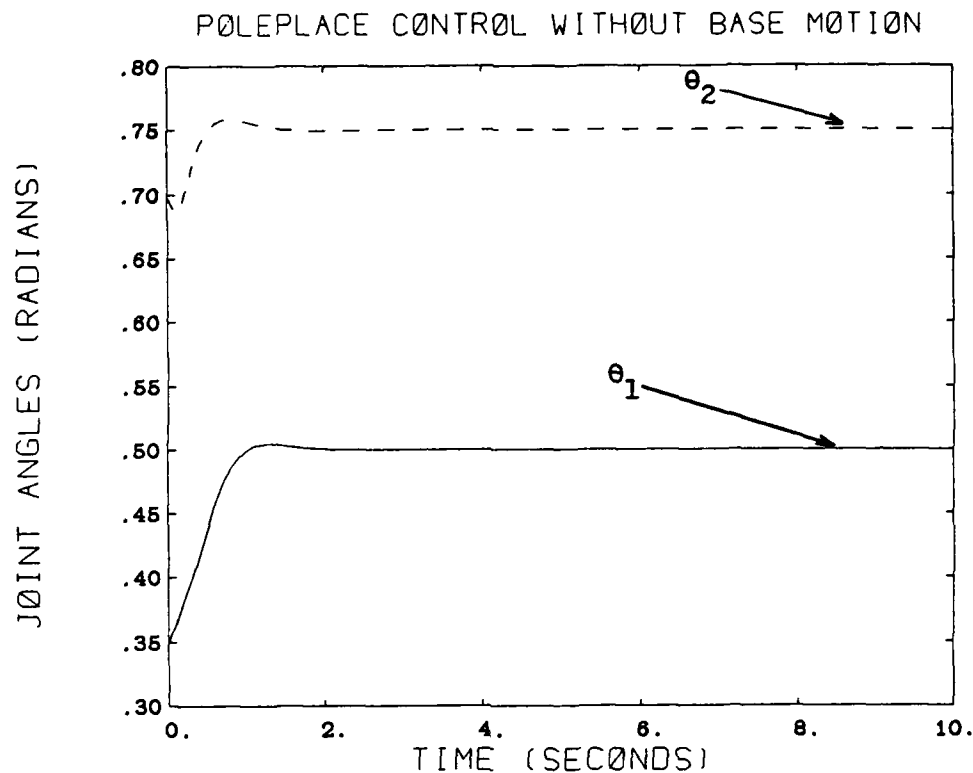


FIGURE 5-10 POLE PLACE CONTROL WITHOUT BASE MOTION

For the purposes of this investigation, this response is acceptable. The speed of response is good, and little overshoot exists. The system obviously is stable.

The question now becomes whether or not this controller can compensate for a base acceleration of the magnitude described in this problem. An additional simulation was then conducted, subjecting the system to a base motion with a base acceleration of at most plus or minus 16 ft/sec^2 . The results were as follow:

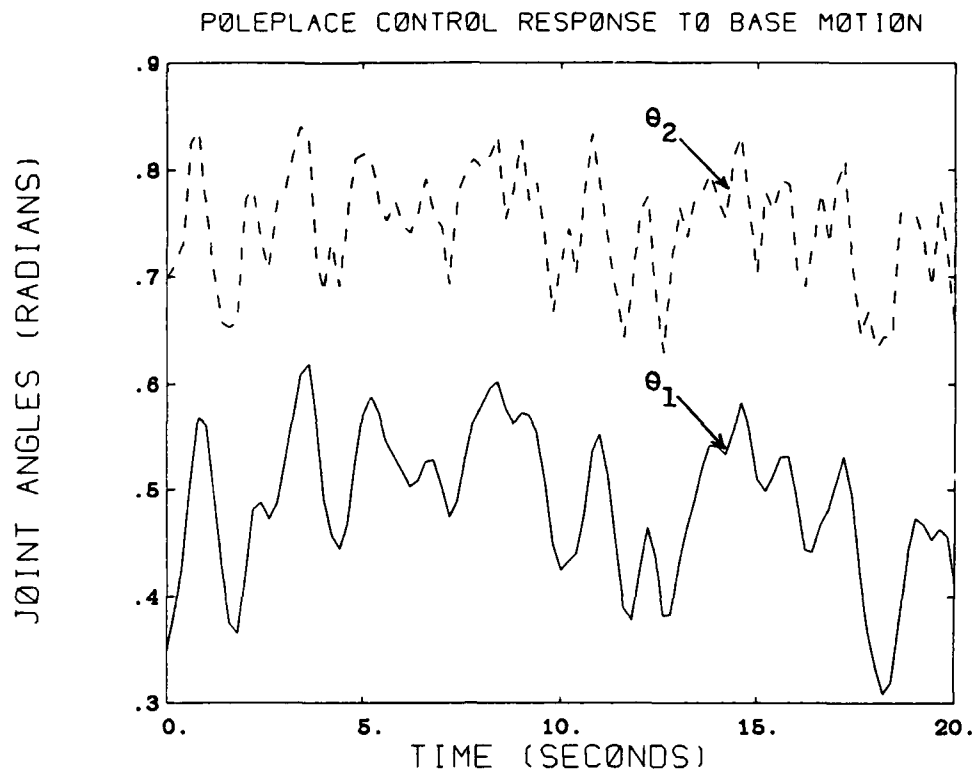


FIGURE 5-11 POLE PLACE CONTROL RESPONSE TO BASE MOTION

This controller was not able to compensate for the motion of the base. The disturbance led to a wildly oscillating system that never reached a stable configuration. An attempt was then made to stabilize this new system by moving the poles farther to the left (and hence increasing required gains), with the following results:

$$\begin{aligned}
 \text{desired pole locations: } p_1 &= -5.0 + 5.0 i \\
 p_2 &= -5.0 - 5.0 i \\
 p_3 &= -15.0 + 15.0 i
 \end{aligned} \tag{5.41}$$

$$p_4 = -15.0 - 15.0 i$$

which led to a gain matrix:

$$\underline{\bar{K}} = \begin{bmatrix} 5498.9 & 1539.50 & 2429.0 & 421.970 \\ -2494.7 & -333.23 & 5702.6 & 40.342 \end{bmatrix} \quad (5.42)$$

and a response as indicated below:

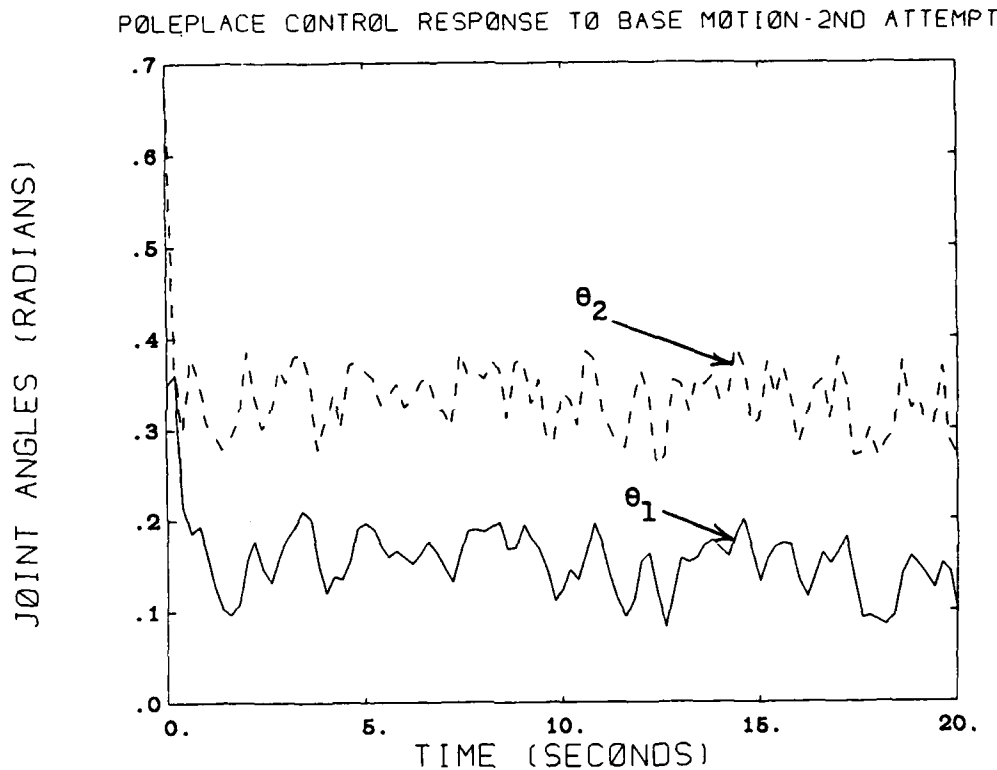


FIGURE 5-12 POLE PLACE CONTROL RESPONSE TO BASE MOTION
2ND ATTEMPT

The increased gains led to an improved, though still unacceptable response when compared to the required specifications for system response. The oscillations have been damped, but an acceptable steady state value is never

obtained. Again moving the poles, and increasing the gains, led to:

$$\begin{aligned} \text{desired pole locations: } p_1 &= -10.0 + 10.0 \\ p_2 &= -10.0 - 10.0 \\ p_3 &= -15.0 + 15.0 \\ p_4 &= -15.0 - 15.0 \end{aligned} \quad (5.43)$$

which led to a gain matrix of:

$$\underline{K} = \begin{bmatrix} 11152.0 & 2140.10 & 5773.6 & 340.78 \\ -5871.0 & -720.90 & 11351.0 & -223.63 \end{bmatrix} \quad (5.44)$$

and a response as indicated below:

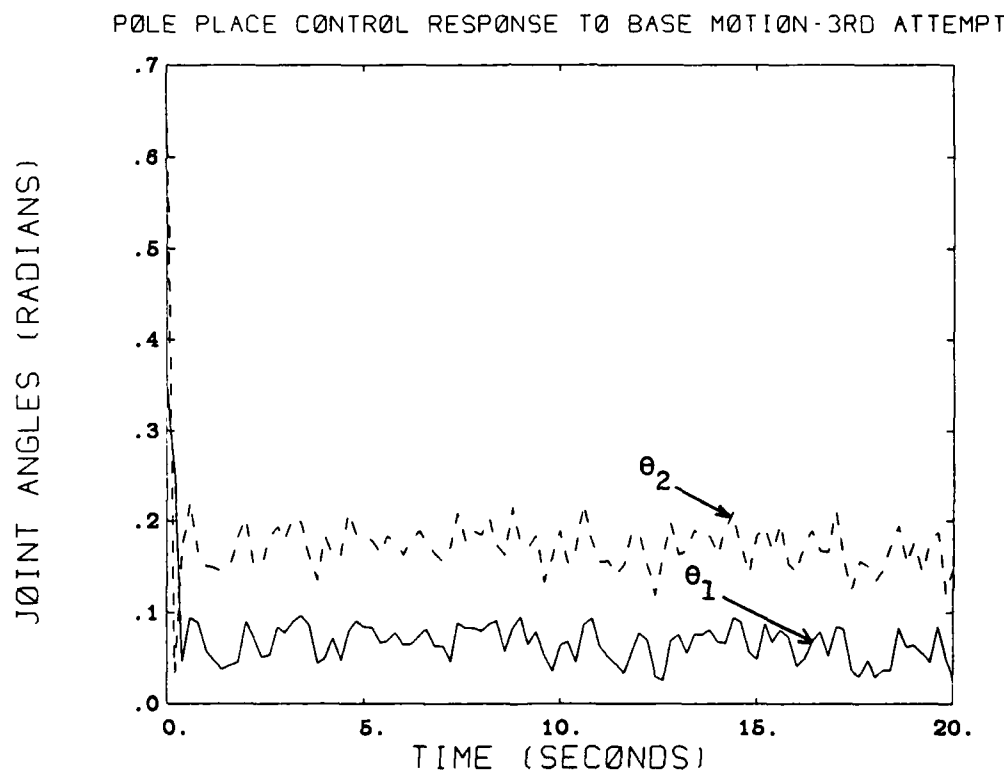


FIGURE 5-13 POLE PLACE CONTROL RESPONSE TO BASE MOTION
THIRD ATTEMPT

Again the response is better, but still not acceptable. It

was found that, as in the case of the PID controller, continuing to increase the gains eventually led to an acceptable, though unrealistic response. Again this is primarily due to bandwidth constraints. Continuing to increase the gains would eventually lead to a controller whose bandwidth exceeded that of the disturbance, but the gains would be so high that actuator saturation, etc. would become a major problem.

5.5 Summary

In this chapter three existing advanced control algorithms (decoupling, LQR and poleplacement) were applied to the moving base problem in an attempt to see if they were robust enough to compensate for the motion of the base. It was found that although they all exhibited a certain amount of disturbance rejection capability, they were not able to reject disturbances of the magnitude under investigation in this research. The bandwidth of the disturbance becomes the dominant factor, and realistic controllers could not be designed that could compensate for the base motion.

CHAPTER 6

NONLINEAR SIMULATION OF POLE PLACE CONTROLLER

6.1 Introduction

Up to this point in the investigation, all simulations have been conducted utilizing linear equations investigating small perturbations around nominal operating values. It is important now to apply the linear controller that proved to be the most effective, the pole place controller, to the nonlinear system with the manipulator operating over its full range of motion. This will provide for insight into the actual system operation.

6.2 Nonlinear simulation results

The pole place controller had the best results in its attempt to compensate for the motion of the base in the linear realm. The results did not meet the system specifications, but were the best of those controllers designed and studied. The linear pole place controller will now be applied to the nonlinear system with the manipulator traversing over its entire range of motion. This simulation will be conducted utilizing the packaged program SIMNON. The SIMNON codes that were prepared for the simulation are listed at APPENDIX A. A fourth order Runge-Katta integration routine was used for the integration.

Simulations were conducted for all of the sets of gains that were designed in Chapter 5 using the pole place technique. In the nonlinear simulations, the manipulator was originally in a configuration where it could feasibly withdraw an ammunition round from the ammunition rack. This configuration led to the following initial conditions:

$$\theta_1^0 = 2.36 \text{ radians}$$

$$\theta_2^0 = 1.80 \text{ radians}$$

The manipulator was commanded to go to a configuration where it could feasibly load ammunition into the gun tube. The desired values for the gun tube then became:

$$\theta_{1d} = .95 \text{ radians} \quad (6.1)$$

$$\theta_{2d} = 0.0 \text{ radians}$$

The simulations were first conducted where the manipulator was assumed to be mounted on a fixed base. The best results were obtained for that set of gains that had the smallest bandwidth (i.e. lowest gains). These were as indicated below:

desired pole locations:

$$\begin{aligned} p_1, p_2 &= -3.0 + 3.0 i \\ p_3, p_4 &= -10.0 + 10.0 i \end{aligned} \quad (6.2)$$

$$\bar{K} = \begin{vmatrix} 1988.4 & 987.43 & 541.43 & 235.98 \\ -576.45 & -90.529 & 2242.2 & 85.686 \end{vmatrix} \quad (6.3)$$

The results of the simulation are as indicated below:

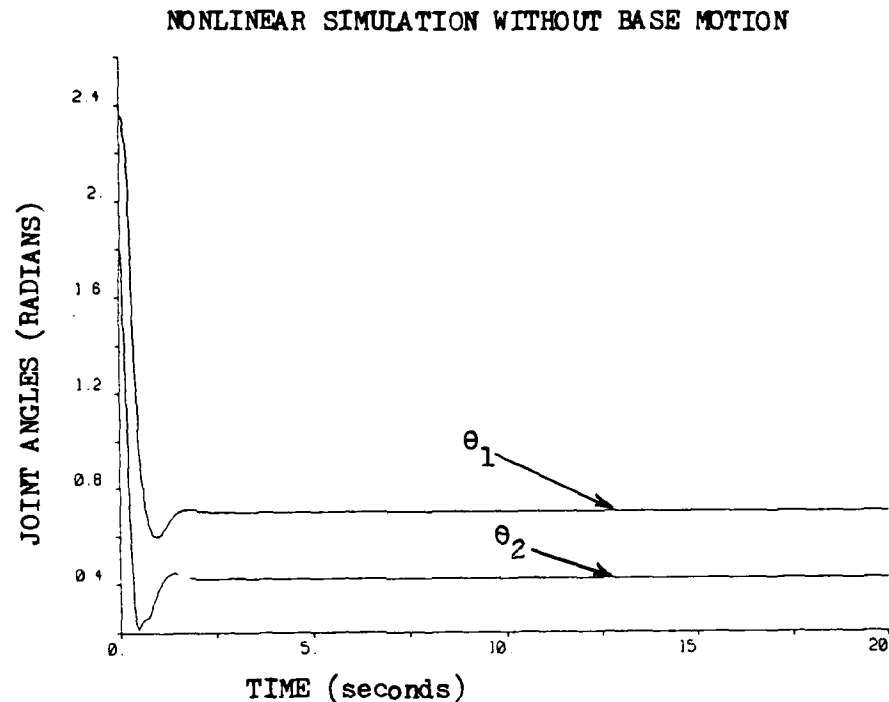


FIGURE 6-1 NONLINEAR SIMULATION WITHOUT BASE MOTION

These results are relatively good. The speed of response is within allowable specifications, as is the system stability. However, in terms of accuracy there exists a steady state error that is outside of allowable limits. This steady state error could be a function of unmodeled system dynamics such as static offset.

The system is now subjected to a base disturbance. In order to investigate disturbances with various bandwidths, sinusoidal inputs were used in the nonlinear simulations to test system response. In the first simulation, the initial

ANALYSIS OF THE DYNAMICS AND CONTROL OF A TWO DEGREE OF
FREEDOM ROBOTIC MANIPULATOR MOUNTED ON A MOVING BASE
(U) ARMY MILITARY PERSONNEL CENTER ALEXANDRIA VA

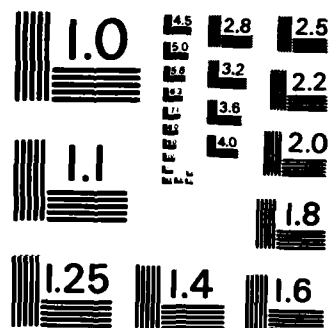
UNCLASSIFIED

R LYNCH 18 OCT 85

F/G 5/8

NL

END



MICROCOPY RESOLUTION TEST CHART
NATIONAL BUREAU OF STANDARDS-1963-A

conditions and desired final values as indicated in equation 6.1. The system is subject to a base acceleration of:

$$y = 16 * \sin(3t)$$

which provides for a disturbance of the magnitude under investigation with a bandwidth of 3 hertz. The results of the simulation are as follows:

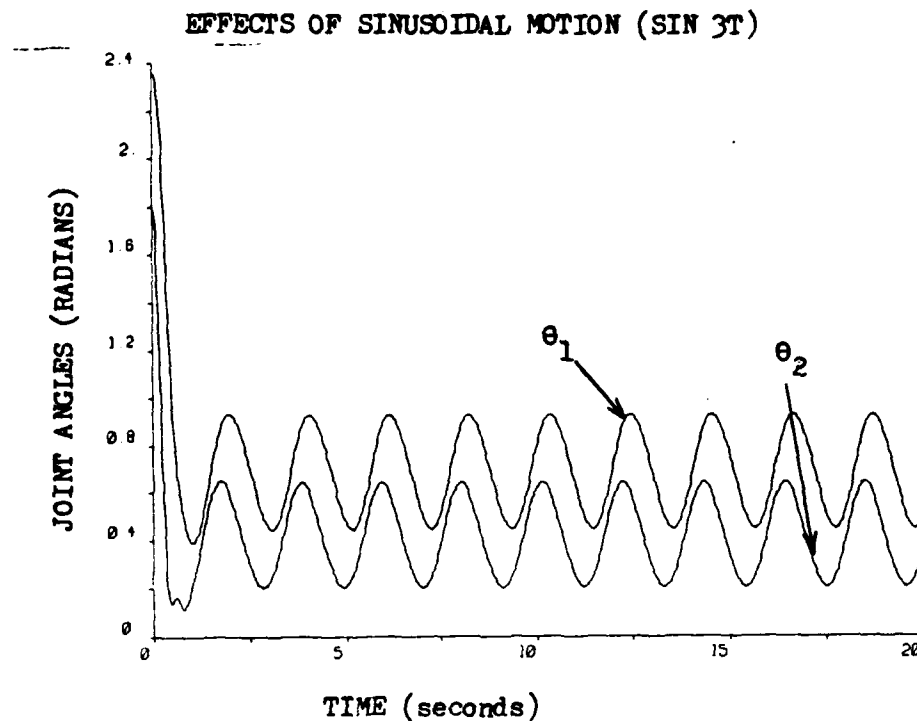


FIGURE 6-2 NONLINEAR SIMULATION WITH BASE MOTION

The system was unable to adequately compensate for the motion of the base. The bandwidth of the disturbance is greater than the bandwidth of the controller.

In the next simulation, the bandwidth of the disturbance was lowered. In this case:

$$y = 16 \sin(t)$$

The results are as follow:

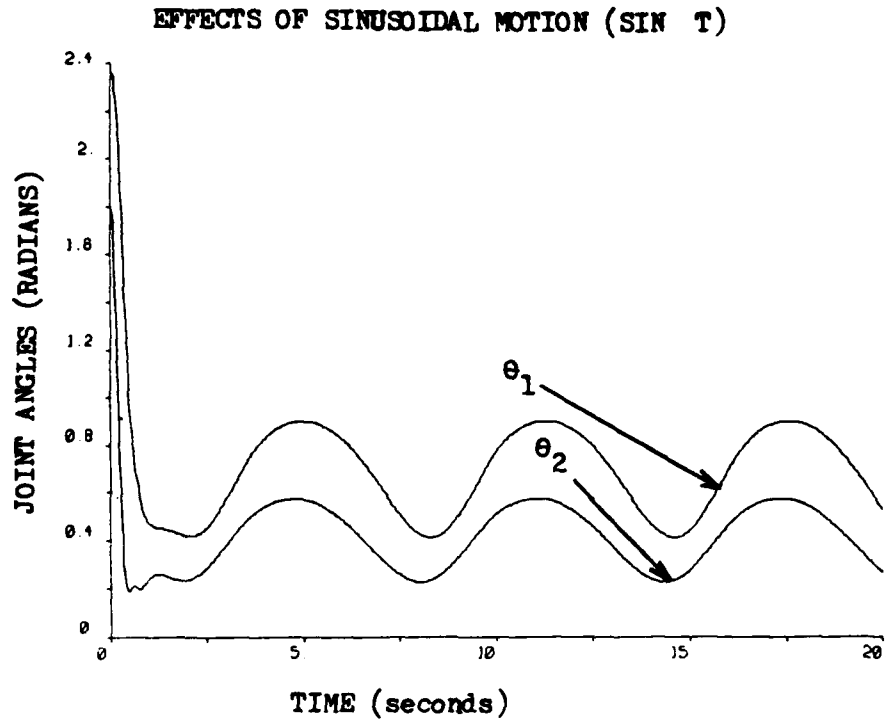


**FIGURE 6-3 NONLINEAR SIMULATION WITH BASE MOTION
SMALLER BANDWIDTH**

As was expected, the controller is better able to compensate for the disturbance of a lower bandwidth. The oscillations are less pronounced, and overall system stability is better.

6.3 Summary

In this chapter a linear controller was applied to the nonlinear system to check for response over the entire range of motion of the manipulator. It was found that, as was the case in the linear controller, the bandwidth of the controller had to be greater than the bandwidth of the disturbance in order to achieve acceptable response.

CHAPTER 7

CONCLUSIONS

It has been shown in this thesis that mounting a manipulator on a moving base does indeed create complications for the dynamics and control of the manipulator. The motion of the base creates disturbances that interfere with the control of the manipulator. If the bandwidth of the disturbances is greater than that of the manipulator controller, then the controller will not be able to compensate for the motion of the base. If the bandwidth of the disturbance is high, as was the case in this thesis, then it is possible that an effective controller cannot be realistically designed to compensate for the base motion. The high bandwidth necessary could only be achieved by extremely high gains, which in turn lead to such problems as actuator saturation, interference with structural resonances of the manipulator, additional noise problems, etc.

Potential solutions to the moving base problem do exist, however. Knowledge of the base motion in terms of sensory information for the controller could allow the controller the capability to compensate for the base motion. This sensory information could either be used in the actual design of the controller, or could be dynamically fed forward using the Luh-Walker-Paul algorithm so that the torques that would be required to compensate for the base motion could be computed and effected.

Another possible solution is the implementation of high quality actuators that could accomodate the gains necessary for a high bandwidth controller. Today's state-of-the-art technology, however, does not provide for actuators that meet this need. Actuators that can accomodate high gains tend to be bulky and slow and would not meet speed of response specifications.

CHAPTER 8

RECOMMENDATIONS FOR FURTHER RESEARCH

This investigation has established the framework for further studies of the moving base problem. It has verified that a problem does indeed exist with mounting a manipulator on a moving base. It has also illustrated that conventional control techniques, along with more advanced control algorithms, are not effective in compensating for the motion of the base.

As was indicated in Chapter 1, research in this area is extremely sparse. With this thesis as a foundation, the following areas should be explored:

- 1) A new algorithm must be developed that will provide for an effective control design that is able to compensate for large base accelerations.
- 2) The model must be expanded from the two link planar model to a three dimensional, multi-degree of freedom manipulator.
- 3) Modeling considerations that were ignored in this study, such as motor inertia , actuator dynamics, etc. must be taken into consideration.
- 4) Detailed computer simulations must be conducted to verify controller effectiveness.

5)Control algorithms must then be applied to actual hardware, as a final verification that they do indeed work.

LIST OF REFERENCES

- [1] "Applications of Robotics and Artificial Intelligence to Reduce Risk and Improve Effectiveness: A Study for the United States Army," Published by the National Academy Press, Washington, D.C. 1983.
- [2] Dubowsky, S., "The Dynamics and Control of Robotic Manipulators," Proceedings of the NATO Advanced Study Institute on Robotics and Artificial Intelligence, Pascoli, Italy, June 1983.
- [3] Rakhmanov, YE.V., Strelkov, A.N., Shvedov, V.N., "Development of a Mathematical Model of a Flexible Manipulator Mounted on a Moving Base," Engineering Cybernetics, Vol. 19, No.4, pp. 81-86, July/Aug 1981.
- [4] Luh, J.Y.S., Walker, M.W., Paul, R.P.C., "On-line Computational Scheme for Mechanical Manipulators," Journal of Dynamic Systems, Measurement, and Control, ASME Trans., Vol. 102, No.2, pp.69-76, June 1980.
- [5] Cannon, R.H., Schmitz, E., "Initial Experiments on the End Point Control of a Flexible One Link Robot", International Journal of Robotics Research, Fall 1984.
- [6] CRC Standard Mathematical Tables, 21st Edition, CRC Press, 1973.
- [7] Lance, G.M., Liang, C., McCleary, M.A., "Integrated Simulation of Vehicular Systems with Stabilization," Proceedings of the Meeting of the Coordinating Group on Modern Control Theory (4th), Rochester, Michigan, 27-28 October 1982.
- [8] Shiller, Z. "Optimal Dynamic Trajectories and Modelling of Robotic Manipulators," M.S. Thesis, M.I.T., Cambridge, Ma., June 1983.
- [9] Kwakernaak, S., Sivan, R., Linear Optimal Control Systems, Wiley Interscience, 1972.
- [10] D'Azzo, J.J., Houpis, H.H., Linear Control System Analysis and Design, Conventional and Modern, McGraw-Hill Book Company, 1981.
- [11] Brady, M. et al., Robot Motion Planning and Control. The MIT Press, 1982.
- [12] Ogata, K., Modern Control Engineering, Prentice-Hall, Inc., 1970.
- [13] Brogan, Modern Control Theory, Prentice-Hall,

Inc., 1982.

[14] Fernandez, B., "POLESYS III User's Manual", MIT. 1984.

[15] Astrom, K., "A Simmon Tutorial", Lund Institute of Technology, 1982.

[16] CTRLC, A Language for the Computer-Aided Design of Multivariable Control Systems, Systems Control Technology, Palo Alto, CA., 1983.

[17] MATRIXX User's Guide, Version 4.0, Integrated Systems, Inc., Palo Alto, CA., 1982.

[18] Crandall, S., Karnopp, D., Kurtz, E., Pridmore-Brown, D., Dynamics of Mechanical and Electromechanical Systems, Robert E. Krieger Publishing Company, Malabar, Florida, 1982.

[19] Rosenberg, R., Karnopp, D., Introduction to Physical System Dynamics, McGraw-Hill, Inc., 1983.

[20] Vukobratovic, M., Potkonjak, V., Dynamics of Manipulation Robots, Theory and Application, Springer-Verlag, Berlin 1982.

[21] Dubowsky, S., A Research Proposal of the Study of The Dynamic Behavior and Control of Mobile Robotic Devices and Manipulators with Potential Application to Military Systems, MIT, 1984.

[22] Lee, C.S.G., Robot Arm Dynamics, IEEE Transactions, 1983.

[23] Golla, D.F., Garg, S.C., and Hughes, P.C. Linear State-Feedback Control of Manipulators, Mechanism and Machine Theory, Vol. 16, pp. 93-103, 1981.

[24] Hedrick, J. Karl, "Notes on the Stability of Linear Systems Designed by Quadratic Synthesis", MIT, 1978.

[25] Paul, R.P., Robot Manipulators: Mathematics, Programming and Control, The MIT Press, 1981.

[26] Slotine, J.J., The Robust Control of Robot Manipulators, International Journal of Robotics Research, 1985.

[27] Wen, J. and Desrochers, A.E., "Control System Design for a Robotic Autoloader". Proceedings of the 23rd Conference on Decision and Control, December 1984.

[28] Kim, S.S., Shabana, A.A., and Haug, E.J., "Automated Vehicle Dynamic Analysis with Flexible Components", Journal of Mechanisms, Transmissions, and Automation in Design, ASME, Vol 106, pp 126-132, March 1984.

[29] Galaitis, A.G., "TRAXION: A Model for Predicting Dynamic Track Loads in Military Vehicles", ASME Journal of Vibration, Acoustics, Stress and Reliability in Design, Vol 106, pp. 286-291, April 1984.

[30] Pavitt, C. ABRAMS Characteristics and Description Book-M1 Tank. General Dynamics Land Systems Division, Aug 1982.

[31] Sandor, G.M. and Erdman, A.G. Advanced Mechanism Design: Analysis and Synthesis Volume 2. Prentice-Hall, Inc. 1984.

[32] Athens, M. "The Role and Use of The Stochastic Linear Quadratic Problem in Control Systems". IEEE Transactions on Automatic Control. Vol AC-16, December 1971.

[33] Berlage, B.L. "Application of Robotics/Smart Machine Technology to Ammunition Handling", Science Application Inc. Technical Memorandum 2-84, February 1984.

APPENDIX A

NON-LINEAR SIMULATION ROUTINES

This appendix contains the routines that were utilized to perform the nonlinear simulations. They were used in conjunction with the packaged program SIMNON.

```

CONTINUOUS SYSTEM MBAS
"THIS PROGRAM CONDUCTS A NONLINEAR SIMULATION OF SYSTEM IN THE
"ABSENCE OF CONTROLS
"INPUT T1 T2 YDD
STATE X1 X2 X3 X4 X5
DER DX1 DX2 DX3 DX4 DX5
S1=SIN(X1)
C1=COS(X1)
S2=SIN(X3)
C2=COS(X3)
S3=SIN(X3-X1)
C3=COS(X3-X1)
M1=9.2
M2=9.93
L1=3.0
L2=3.0
L1C=1.53
L2C=1.88
J1=6.44
J2=5.11
G=0.0
T1=0.0
T2=0.0
YDD=1.0
A=M1*L1C*L1C+J1+M2*L1*L1
B=M2*L1*L2C*C3
C=M1*L1C*C1+M2*L1*C1
D=M2*L2C*L1*S3
E=M1*L1C*C1+M2*L1*C1
F=M1*L1C*S1*X5*X2
H=M2*L2C*L2C+J2
K=M2*L2C*C2
R=T1-T2-C*YDD+D*X4*X4-E*G+F
S=T2-K*YDD-D*X2*X2-K*G
DX1=X2
DX2=(R*H-B*S)/(A*H-B*B)
DX3=X4
DX4=(S*A-B*R)/(A*H-B*B)
DX5=YDD
END

```



```
CONTINUOUS SYSTEM SYST
INPUT U1 U2 YDD
OUTPUT Y1 Y2 Y3 Y4 Y5
STATE X1 X2 X3 X4 X5
DER DX1 DX2 DX3 DX4 DX5
S1=SIN(X1)
C1=COS(X1)
S2=SIN(X3)
C2=COS(X3)
S3=SIN(X3-X1)
C3=COS(X3-X1)
M1=9.2
M2=9.93
L1=3.0
L2=3.0
L1C=1.53
L2C=1.88
J1=6.44
J2=5.11
G=-32.2
A=M1*L1C*L1C+J1+M2*L1*L1
B=M2*L1*L2C*C3
C=M1*L1C*C1+M2*L1*C1
D=M2*L2C*L1*S3
E=M1*L1C*C1+M2*L1*C1
F=M1*L1C*S1*X5*X2
H=M2*L2C*L2C+J2
K=M2*L2C*C2
R=U1-U2-C*YDD+D*X4*X4-E*G+F
S=U2-K*YDD-D*X2*X2-K*G
DX1=X2
DX2=(R*H-B*S)/(A*H-B*B)
DX3=X4
DX4=(S*A-B*R)/(A*H-B*B)
DX5=YDD
Y1=X1
Y2=X2
Y3=X3
Y4=X4
Y5=X5
END
```

DISCRETE SYSTEM REGNON
" THIS FILE CONTAINS THE POLE PLACE CONTROL CODE
INPUT R1 R2 Y1 Y2 Y3 Y4 Y5
OUTPUT U1 U2 YDD
TIME T
TSAMP TS
 $U1 = R1 - ((K1 * Y1) + (K2 * Y2) + (K3 * Y3) + (K4 * Y4))$
 $U2 = R2 - ((K5 * Y1) + (K6 * Y2) + (K7 * Y3) + (K8 * Y4))$
OMG=3
 $YDD = 16 * SIN(T)$
 $TS = T + H$
H:.05
K1=1988.4
K2=987.43
K3=541.43
K4=235.98
K5=-576.45
K6=-90.529
K7=2242.2
K8=85.686
END

CONNECTING SYSTEM CREGNON

" THIS FILE CONTAINS THE CONNECTOR FOR THE CONTROLLER/SYSTEM

R1[REGNON]=.95

R2[REGNON]=0

Y1[REGNON]=Y1[SYST]

Y2[REGNON]=Y2[SYST]

Y3[REGNON]=Y3[SYST]

Y4[REGNON]=Y4[SYST]

Y5[REGNON]=Y5[SYST]

U1[SYST]=U1[REGNON]

U2[SYST]=U2[REGNON]

YDD[SYST]=YDD[REGNON]

END

APPENDIX B

LINEARIZATION SPECIFICS

This appendix contains the linearized equations of motion for a two degree of freedom planar manipulator. The linearization procedure used was as described in Chapter 3. In addition, this appendix also contains the FORTRAN code for the program LINEAR which was written to expedite the linearization process.

The following are the linearized equations of motion:

EQUATION 1

$$\begin{aligned}
 T_1 - T_2 &= (m_1^2 + m_2^2 + J_1) \ddot{\theta}_1 + (m_2 L_2 \cos \theta_2 \cos \theta_1^{\cdot}) \ddot{\theta}_2 \\
 &+ m_2 L_2 \sin \theta_2 \sin \theta_1^{\cdot} \ddot{\theta}_1 - (m_1 \dot{y}_1 \sin \theta_1^{\cdot}) \dot{\theta}_1 \\
 &+ (2m_2 L_2 \dot{\theta}_2 \cos \theta_2 \sin \theta_1^{\cdot} - 2m_2 L_2 \sin \theta_2 \cos \theta_1^{\cdot} \dot{\theta}_2) \dot{\theta}_1 \\
 &+ (m_2 L_2 \ddot{\theta}_2 \sin \theta_2 \cos \theta_1^{\cdot} - m_2 L_2 \ddot{\theta}_2 \cos \theta_2 \sin \theta_1^{\cdot}) \\
 &- m_1 \dot{y}_1 \cos \theta_1^{\cdot} \dot{\theta}_1 + m_2 L_2 \dot{\theta}_2 \dot{\theta}_1 \sin \theta_2 \sin \theta_1^{\cdot} \\
 &+ m_2 L_2 \dot{\theta}_2 \dot{\theta}_1 \cos \theta_2 \cos \theta_1^{\cdot} - m_1 g \sin \theta_1^{\cdot} - m_2 L_2 g \sin \theta_2^{\cdot} \\
 &- m_1 \ddot{y}_1 \sin \theta_1^{\cdot} - m_2 L_2 \sin \theta_2^{\cdot} \ddot{y}_1 \dot{\theta}_1 + (m_2 L_2 \ddot{\theta}_2 \cos \theta_2 \sin \theta_1^{\cdot}) \\
 &- m_2 L_2 \ddot{\theta}_2 \sin \theta_2 \cos \theta_1^{\cdot} - m_2 L_2 \dot{\theta}_2 \dot{\theta}_1 \cos \theta_2 \cos \theta_1^{\cdot} \\
 &- m_2 L_2 \dot{\theta}_2 \dot{\theta}_1 \sin \theta_2 \sin \theta_1^{\cdot} \dot{\theta}_1 + (m_2 L_2 \cos \theta_2^{\cdot}) \\
 &+ m_2 L_2 \cos \theta_2^{\cdot} \ddot{y}_1 - (m_1 \sin \theta_1^{\cdot} \dot{\theta}_1^{\cdot}) \dot{y}_1
 \end{aligned}$$

EQUATION 2

$$\begin{aligned}
T_2 = & \left(m L_1 \cos \theta_1 \cos \theta_2 + m L_1 \sin \theta_1 \sin \theta_2 \right) \delta \ddot{\theta}_1 \\
& + \left(m \frac{L_1^2}{2} + J_2 \right) \delta \ddot{\theta}_2 + \left(2 m L_1 \dot{\theta}_1 \sin \theta_1 \cos \theta_2 \right. \\
& - 2 m L_1 \dot{\theta}_1 \cos \theta_1 \sin \theta_2 \left. \right) \delta \dot{\theta}_1 + \left(m L_1 \ddot{\theta}_1 \sin \theta_1 \cos \theta_2 \right. \\
& - m L_1 \ddot{\theta}_1 \cos \theta_1 \sin \theta_2 - m L_1 \dot{\theta}_1 \dot{\theta}_2 \sin \theta_1 \sin \theta_2 \\
& - m L_1 \dot{\theta}_1 \dot{\theta}_2 \cos \theta_1 \cos \theta_2 \left. \right) \delta \theta_1 + \left(m L_1 \ddot{\theta}_1 \cos \theta_1 \sin \theta_2 \right. \\
& - m L_1 \ddot{\theta}_1 \sin \theta_1 \cos \theta_2 - m \frac{L_1^2}{2} \ddot{\theta}_2 \sin \theta_2 - m g L_1 \sin \theta_2 \\
& - m L_1 \dot{\theta}_1 \dot{\theta}_2 \cos \theta_1 \cos \theta_2 + m L_1 \dot{\theta}_1 \dot{\theta}_2 \sin \theta_1 \sin \theta_2 \left. \right) \delta \theta_2 \\
& + \left(m \frac{L_1^2}{2} \cos \theta_2 \right) \ddot{y}
\end{aligned}$$

PROGRAM LINEAR

```

cccccccccccccccccccccccccccccccccccccccccccccccccccccccccccc
real t(2),td(2),tdd(2),z(2),zd(2),zdd(2),const,m1,m2,
real l2c,j1,j2,x1,x2,xld,x2d,xldd,x2dd,y1,y2,ydd,yd
c   variables are:
c   x1=theta one nominal
c   x2=theta two nominal
c   xld=nominal link one velocity
c   x2d=nominal link two velocity
c   xldd=nominal link one acceleration
c   x2dd=nominal link two acceleration
c   y1=nominal base velocity
c   y2=nominal base acceleration
g=-32.2
m1=9.2
m2=9.93
l1=3.0
l2=3.0
l1c=1.53
l2c=1.88
j1=6.44
j2=5.11
x1=2.36
x2=1.83
xld=1.0
x2d=1.0
xldd=1.0
x2dd=1.0
y1=1.0
y2=1.0

c
c   Coefficients for equation #1
tdd(1)=m1*l1c*l1c+j1+m2*l1*l1
tdd(2)=m2*l1*l2c*cos(x2)*cos(x1)+m2*l1*l2c*sin(x2)*sin(x1)
td(1)=-m1*l1c*y1*sin(x1)
td(2)=-2*m2*l1*l2c*x2d*sin(x2)*cos(x1)+2*m2*l1*l2c*x2d*cos(x2)
1   *sin(x1)
t(1)=-m2*l1*l2c*x2dd*cos(x2)*sin(x1)+m2*l1*l2c*x2dd*sin(x2)
1   *cos(x1)-m1*l1c*y2*sin(x1)-m2*l1*y2*sin(x1)-m1*g*l1c*sin(x1)
1   -m2*g*l1*sin(x1)-m1*l1c*y1*cos(x1)*xld+m2*l1*l2c*x2d*x2d
1   *sin(x2)*sin(x1)+m2*l1*l2c*x2d*x2d*cos(x2)*cos(x1)
t(2)=-m2*l1*l2c*x2dd*sin(x2)*cos(x1)+m2*l1*l2c*cos(x2)
1   *sin(x1)-m2*l1*l2c*x2d*x2d*cos(x2)*cos(x1)-m2*l1*l2c
1   *x2d*x2d*sin(x2)*sin(x1)
yd=-m1*l1c*sin(x1)*xld
ydd=m1*l1c*cos(x1)+m2*l1*cos(x1)
type *, 'coefficients for the first equation'
type *, 'tdd(1)=',tdd(1), 'tdd(2)=',tdd(2)
type *, 'td(1)=',td(1), 'td(2)=',td(2)
type *, 't(1)=',t(1), 't(2)=',t(2)
type *, 'yd=',yd, 'ydd=',ydd

```

c Coefficients for equation #2

```

      zdd(1)=+m2*l1*l2c*cos(x2)*cos(x1)+m2*l1*l2c*sin(x2)
1      *sin(x1)
      zdd(2)=m2*l2c*l2c+j2
      zd(1)=2*m2*l1*l2c*xld*sin(x2)*cos(x1)-2*m2*l1*l2c*xld
1      *cos(x2)*sin(x1)
      z(1)=-m2*l1*l2c*xldd*cos(x2)*sin(x1)+m2*l1*l2c*xldd*sin(x2)
1      *cos(x1)-m2*l1*l2c*xld*xld*sin(x2)*sin(x1)-m2*l1*l2c
1      *xld*xld*cos(x2)*cos(x1)
      z(2)=-m2*l1*l2c*xldd*sin(x2)*cos(x1)+m2*l1*l2c*xldd
1      *cos(x2)*sin(x1)-m2*l2c*g*sin(x2)-m2*l2c*y2*sin(x2)
1      -m2*l1*l2c*xld*xld*cos(x2)*cos(x1)+m2*l1*l2c*xld
1      *xld*sin(x2)*sin(x1)
      ydd2=m2*l2c*cos(x2)
      type *, 'coefficients for the second equation'
      type *, 'zdd(1)=', zdd(1), 'zdd(2)=', zdd(2)
      type *, 'zd(1)=', zd(1), 'zd(2)=', zd(2)
      type *, 'z(1)=', z(1), 'z(2)=', z(2)
      type *, 'yd2=', yd2, 'ydd2=', ydd2
      stop
      end

```


APPENDIX C
POLESYS3 ROUTINES

This appendix contains an example of a POLESYS3 program run which was used to place the poles of this multi-input, multi-output system.

POLESYS III : Optimal Output Feedback Control Design usign
 Pole_placement Techniques and Minimal Gain/Maximal decoupling
 (c) 1984, Benito FERNANDEZ R. [M.I.T. / M.E. Department]
 Running at the JCF / M.I.T. Date: 2-SEP-85 Time: 06:24:22

Job Title: FILE INPUT

Logical Unit Input: 1 Input File Name : CASE1.DAT

Logical Unit Output: 2 Output File Name : CASE111.OUT

Number of States NX: 4

Number of Meassurements NY: 2

Number of Controls NU: 2

Number of Perturbations NW: 0

State Feedback control Design

States Poles_Placement Design

A matrix

0.00000D+00	0.10000D+01	0.00000D+00	0.00000D+00
-0.11790D+02	0.11300D+01	0.10330D+02	0.79100D+00
0.00000D+00	0.00000D+00	0.00000D+00	0.10000D+01
0.16210D+02	-0.24300D+01	-0.21600D+02	-0.10300D+01

B matrix

0.00000D+00	0.00000D+00
0.21000D-01	-0.48000D-01
0.00000D+00	0.00000D+00
-0.28000D-01	0.89000D-01

C matrix

0.10000D+01	0.00000D+00	0.00000D+00	0.00000D+00
0.00000D+00	0.00000D+00	0.10000D+01	0.00000D+00

D matrix

0.00000D+00	0.00000D+00
0.00000D+00	0.00000D+00

Desired Closed-loop Eigenvalues

-0.10000D+02	0.10000D+02
-0.10000D+02	-0.10000D+02
-0.15000D+02	0.15000D+02
-0.15000D+02	-0.15000D+02

POLESYS III >System Entering Optimization Sequence

Overall Transformation Matrix, T

0.10000D+01	0.00000D+00	0.00000D+00	0.00000D+00
0.00000D+00	0.10000D+01	0.00000D+00	0.00000D+00
0.00000D+00	0.00000D+00	0.10000D+01	0.00000D+00
0.00000D+00	0.00000D+00	0.00000D+00	0.10000D+01

A matrix

0.00000D+00	0.10000D+01	0.00000D+00	0.00000D+00
-0.11790D+02	0.11300D+01	0.10330D+02	0.79100D+00
0.00000D+00	0.00000D+00	0.00000D+00	0.10000D+01
0.16210D+02	-0.24300D+01	-0.21600D+02	-0.10300D+01

B matrix

0.00000D+00	0.00000D+00
0.21000D-01	-0.48000D-01
0.00000D+00	0.00000D+00
-0.28000D-01	0.89000D-01

C matrix

0.10000D+01	0.00000D+00	0.00000D+00	0.00000D+00
0.00000D+00	0.00000D+00	0.10000D+01	0.00000D+00

D matrix

0.00000D+00	0.00000D+00
0.00000D+00	0.00000D+00

Convergence criterion for estimates

0.10000D-03

Convergence criterion for functions

0.10000D-03

Convergence criterion for gradient

0.10000D-03

Number of iterations allowed, MIA

7777

Machine precision, EPSMCH

0.10000D-09

Machine precision, DWARF

0.10000D-09

POLESYS III >Minimal Gain State-Feedback Control Calculation Starts

Initial E_2_star

0.10000D+01
0.20000D+01
0.30000D+01
0.40000D+01
0.50000D+01
0.60000D+01
0.70000D+01
0.80000D+01

POLESYS III >*** CHECK DIAGNOSTIC REPORT ***

Sum of Squares, SSQ1

0.10000D-03

POLESYS III >*** SUCCESSFUL COMPLETION ***

POLESYS III >Both Actual and Predicted Relative Reductions in the sum of
POLESYS III >squares are at most SSQ1

Original Space Control Gain Matrix

0.11152D+05	0.21401D+04	0.57736D+04	0.34078D+03
-0.58710D+04	-0.72090D+03	0.11351D+05	-0.22363D+03

Feedback Control Gain

0.11152D+05	0.21401D+04	0.57736D+04	0.34078D+03
-0.58710D+04	-0.72090D+03	0.11351D+05	-0.22363D+03

(Ad = A - B*CoGain) matrix

0.00000D+00	0.10000D+01	0.00000D+00	0.00000D+00
-0.52779D+03	-0.78415D+02	0.43392D+03	-0.17100D+02
0.00000D+00	0.00000D+00	0.00000D+00	0.10000D+01
0.85099D+03	0.12165D+03	-0.87015D+03	0.28415D+02

Closed-loop Eigenvalues

-0.15000D+02	0.15000D+02
-0.15000D+02	-0.15000D+02
-0.10000D+02	0.10000D+02
-0.10000D+02	-0.10000D+02

Minimal Control Gain, Kx

0.11152D+05	0.21401D+04	0.57736D+04	0.34078D+03
-0.58710D+04	-0.72090D+03	0.11351D+05	-0.22363D+03

Original Space Control Gain Matrix

0.11152D+05	0.21401D+04	0.57736D+04	0.34078D+03
-0.58710D+04	-0.72090D+03	0.11351D+05	-0.22363D+03

Feedback Control Gain

0.11152D+05	0.21401D+04	0.57736D+04	0.34078D+03
-0.58710D+04	-0.72090D+03	0.11351D+05	-0.22363D+03

(Ad = A - B*CoGain) matrix

0.00000D+00	0.10000D+01	0.00000D+00	0.00000D+00
-0.52779D+03	-0.78415D+02	0.43392D+03	-0.17100D+02
0.00000D+00	0.00000D+00	0.00000D+00	0.10000D+01
0.85099D+03	0.12165D+03	-0.87015D+03	0.28415D+02

Closed-loop Eigenvalues

-0.15000D+02	0.15000D+02
--------------	-------------

```

-0.15000D+02  -0.15000D+02
-0.10000D+02   0.10000D+02
-0.10000D+02  -0.10000D+02

```

OPTIMO::>Final Control Gain Matrix

```

  0.11152D+05  0.21401D+04  0.57736D+04  0.34078D+03
-0.58710D+04 -0.72090D+03  0.11351D+05 -0.22363D+03

```

Feedback Control Gain

```

  0.11152D+05  0.21401D+04  0.57736D+04  0.34078D+03
-0.58710D+04 -0.72090D+03  0.11351D+05 -0.22363D+03

```

(Ad = A - B*CoGain) matrix

```

  0.00000D+00  0.10000D+01  0.00000D+00  0.00000D+00
-0.52779D+03 -0.78415D+02  0.43392D+03 -0.17100D+02
  0.00000D+00  0.00000D+00  0.00000D+00  0.10000D+01
  0.85099D+03  0.12165D+03 -0.87015D+03  0.28415D+02

```

Closed-loop Eigenvalues

```

-0.15000D+02  0.15000D+02
-0.15000D+02 -0.15000D+02
-0.10000D+02  0.10000D+02
-0.10000D+02 -0.10000D+02

```

POLESYS III >End of POLESYS III Run

END

FILMED

12-85

DTIC